

# Metal Complexes with Cis $\alpha$ Topology from Stereoselective Quadridentate Ligands with Amine, Pyridine, and Quinoline Donor Groups

Christina Ng, Michal Sabat, and Cassandra L. Fraser\*

Department of Chemistry, University of Virginia, McCormick Road, Charlottesville, Virginia 22901

Received May 4, 1999

Though the principles governing quadridentate topology and metal stereochemistry have been known for some time, the cis  $\alpha$  topology has been little exploited in designing catalysts for asymmetric reactions. Investigation of the inorganic chemistry of labile metal cis  $\alpha$  complexes was undertaken as a prelude to exploring their potential to serve as catalysts for a variety of different reactions. The synthesis of a series of first row transition metal complexes of quadridentate ligands with ethylenediamine (en) and *S*-propylenediamine (*S*-pn) backbones that have been alkylated at nitrogen with either pyridine (py) or quinoline (qn) donor groups as well as with noncoordinating benzyl (Bn) or pentafluorobenzyl (F<sub>5</sub>Bn) groups was undertaken. The steric and electronic properties vary throughout the ligand series, en(Bn)py, **1**, en(F<sub>5</sub>Bn)py, **2**, *S*-pn(F<sub>5</sub>Bn)py, **3**, and *S*-pn(F<sub>5</sub>Bn)qn, **4**. These ligands were reacted with MCl<sub>*n*</sub> salts (*n* = 2, M = Mn, Fe, Co, Ni, Cu, Zn; *n* = 3, M = Fe) to generate, in most cases, octahedral complexes with the targeted cis  $\alpha$  topology. UV/vis, NMR, IR, cyclic voltammetry (CV), and conductivity analysis are described for the metal compounds. X-ray structural analysis of [Cu{en(F<sub>5</sub>-Bn)py}Cl]Cl reveals a five coordinate square pyramidal geometry. Single or major diastereomers were obtained for all diamagnetic Zn(II) complexes as well as for Co(III) analogues that were prepared by oxidation of Co(II) species using Br<sub>2</sub> as the oxidant. Electronic differences among ligands are reflected in the oxidation potentials of the respective metal complexes as determined by CV, with fluorinated systems showing greater resistance to oxidation, as expected.

## Introduction

Recently there has been a resurgence of interest in chiral coordination compounds with nitrogen ligands<sup>1–4</sup> for their potential as asymmetric catalysts in both small molecule and polymer synthesis. For example, chiral metal salen analogues have been utilized as asymmetric oxygen<sup>1–8</sup> and nitrogen atom transfer catalysts<sup>5,9,10</sup> and as catalysts for the ring opening of epoxides (Figure 1).<sup>11,12</sup> Complexes of oxazoline ligands, such as pybox, are effective Lewis acid catalysts and promote cyclopropanation and aziridination reactions.<sup>13–21</sup> Osmium–

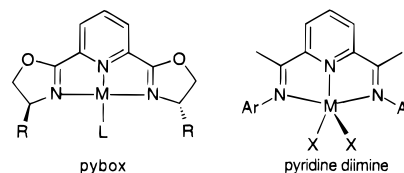
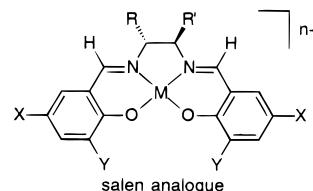


**Figure 1.** Examples of coordination compounds with chelating nitrogen donor ligands used in catalysis.

alkaloid systems have been developed into highly selective catalysts for dihydroxylation<sup>22–24</sup> and aminohydroxylation.<sup>25</sup> Interestingly, simple coordination compounds are also playing key roles as catalysts in contemporary polymer chemistry. Atom

- Ojima, I., Ed. *Catalytic Asymmetric Synthesis*; VCH: New York, 1993.
- Lucet, D.; Le Gall, T.; Mioskowski, C. *Angew. Chem., Int. Ed. Engl.* **1998**, *37*, 2580–627.
- Togni, A.; Venanzi, A. *Angew. Chem., Int. Ed. Engl.* **1994**, *33*, 497–526.
- Wills, M. J. *Chem. Soc., Perkin Trans. 1* **1998**, 3101–20.
- Canali, L.; Sherrington, D. C. *Chem. Soc. Rev.* **1999**, *28*, 85–93.
- Palucki, M.; Finney, N. S.; Pospisil, P. J.; Guler, M. L.; Ishida, T.; Jacobsen, E. N. *J. Am. Chem. Soc.* **1998**, *120*, 948–54 and references therein.
- Chang, S.; Lee, N.; Jacobsen, E. N. *J. Org. Chem.* **1993**, *58*, 6939–41.
- Brandes, B. D.; Jacobsen, E. N. *J. Org. Chem.* **1994**, *59*, 4378–80.
- Hansen, K. B.; Leighton, J. L.; Jacobsen, E. N. *J. Am. Chem. Soc.* **1996**, *118*, 10924–5.
- Konsler, R. G.; Karl, J.; Jacobsen, E. N. *J. Am. Chem. Soc.* **1998**, *120*, 10780–1.
- Du Bois, J.; Tomooka, C. S.; Hong, J.; Carreira, E. M. *Acc. Chem. Res.* **1997**, *30*, 364–72.
- Minakata, S.; Ando, T.; Nishimura, M.; Ryu, I.; Komatsu, M. *Angew. Chem., Int. Ed. Engl.* **1998**, *37*, 3392–4.
- Ghosh, A. K. *Tetrahedron Asymmetry* **1998**, *9*, 1–45.
- Lewis acids: Evans, D. A.; Olhava, E. J.; Johnson, J. S.; Janey, J. M. *Angew. Chem., Int. Ed. Engl.* **1998**, *37*, 3372–5 and references therein.
- Yao, S.; Johannsen, M.; Hazell, R. G.; Jorgensen, K. A. *Angew. Chem., Int. Ed. Engl.* **1998**, *37*, 3121–4.

- Cyclopropanation: Doyle, M. P.; Protopopova, M. N. *Tetrahedron* **1998**, *54*, 7919–46.
- Doyle, M. P.; Forbes, D. C. *Chem. Rev.* **1998**, *98*, 911–35.
- Harm, A. M.; Knight, J. G.; Stemp, G. *Synlett* **1996**, 677–8.
- Denmark, S. E.; Stavenger, R. A.; Faucher, A.-M.; Edwards, J. P. *J. Org. Chem.* **1997**, *62*, 3375–89.
- Bedekar, A. V.; Koroleva, E. B.; Anderson, P. G. *J. Org. Chem.* **1997**, *62*, 2518–26.
- Aziridination: Evans, D. A.; Faul, M. M.; Bilodeau, M. T.; Anderson, B. A.; Barnes, D. M. *J. Am. Chem. Soc.* **1993**, *115*, 5328–9.
- Becker, H.; Sharpless, K. B. *Angew. Chem., Int. Ed. Engl.* **1996**, *35*, 448–51.
- Kolb, H. C.; VanNieuwenhze, M. S.; Sharpless, K. B. *Chem. Rev.* **1994**, *94*, 2483–547.

transfer radical polymerization (ATRP) of styrene and acrylate monomers<sup>26</sup> utilizes Cu(I) complexes with bipyridine,<sup>26–28</sup> chelating amine,<sup>29–31</sup> and Schiff base ligands,<sup>32–34</sup> whereas metal complexes with diimine ligands figure prominently in recent advances in a polyolefin synthesis, with many showing high catalytic activity.<sup>35–37</sup> Chiral variants of some of these systems have been employed in an attempt to control polymer tacticity.<sup>38</sup>

Though systematic catalyst tuning can be difficult for asymmetric complexes possessing  $C_1$  symmetry, numerous derivatives of the dissymmetric  $C_2$ -symmetric quadridentate salen<sup>1–8</sup> and bi- or tridentate oxazoline-based systems<sup>13–21</sup> are known. Upon coordination, these ligands typically adopt planar topologies in which carbon stereocenters on the ligand framework generate a chiral array at the reactive center. Though much success has been achieved with these planar catalysts, comparatively little has been reported about the reactivity of nonplanar chiral chelates despite the fact that methods for controlling linear quadridentate chelate topology and metal absolute configuration have been known for some time. Many studies have been performed using nitrogen donor ligands,<sup>39,40</sup> with mixed pyridylamine chelates figuring prominently.<sup>41</sup> Structural features and physical characterization of many inert and labile metal pyridylamine systems have been investigated.<sup>42–49</sup> This family of ligands has been exploited in bimetallic enzyme

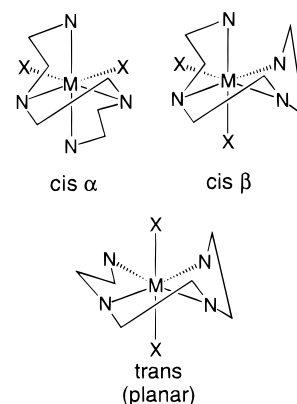


**Figure 2.** Quadridentate chelate topologies.

models<sup>50–54</sup> and as catalysts for redox processes<sup>55–58</sup> and olefin polymerization.<sup>59</sup>

By the appropriate selection of metal chelate ring sizes, donor groups, and chiral centers on the ligand backbone, it is possible to generate ligands that result in major, if not single diastereomers upon coordination to metal ions. Since five-membered chelate rings typically possess bite angles of less than  $90^\circ$ , cumulative angle strain is minimized when chelate rings are positioned out of plane with respect to each other.<sup>60</sup> Others have pointed out that “B strain,” namely unfavorable in-plane nonbonding interactions between  $\alpha$ -hydrogens on pyridyl residues, also disfavor the planar orientation.<sup>43</sup> Thus, quadridentate chelates with three consecutive five-membered metal chelate rings preferentially adopt cis topologies, either cis  $\alpha$  or cis  $\beta$ , over trans structures (Figure 2). For quadridentates in which the two internal donor groups are secondary amines, cis  $\beta$  complexes or mixtures of cis  $\alpha$  and cis  $\beta$  isomers are typically obtained.<sup>41,43,50,61–64</sup> However, when these internal donor groups are tertiary amines<sup>50</sup> or sulfides,<sup>65–67</sup> cis  $\alpha$  structures have been observed. It is assumed that apical binding is energetically preferable to the cis  $\beta$  in-plane chelation, since the terminal

- (24) Norrby P.-O.; Becker, H.; Sharpless, K. B. *J. Am. Chem. Soc.* **1996**, *118*, 35–42.
- (25) Bruncko, M.; Schlingloff, G.; Sharpless, K. B. *Angew. Chem., Int. Ed. Engl.* **1997**, *36*, 1483–6.
- (26) Patten, T. E.; Matyjaszewski, K. *Adv. Mater.* **1998**, *10*, 901–15.
- (27) Matyjaszewski, K.; Patten, T. E.; Xia, J. *J. Am. Chem. Soc.* **1997**, *119*, 9, 674–80.
- (28) Matyjaszewski, K.; Wang, J.-L.; Grimaud, T.; Shipp, D. A. *Macromolecules* **1998**, *31*, 1527–34.
- (29) Xia, J.; Matyjaszewski, K. *Macromolecules* **1999**, *32*, 2434–7.
- (30) Xia, J.; Gaynor, S. G.; Matyjaszewski, K. *Macromolecules* **1998**, *31*, 5958–9.
- (31) Xia, J.; Matyjaszewski, K. *Macromolecules* **1997**, *30*, 7697–700.
- (32) Haddleton, D. M.; Crossman, M. C.; Dana, B. H.; Duncalf, D. J.; Heming, A. M.; Kukulj, D.; Shooter, A. J. *Macromolecules* **1999**, *32*, 2110–9.
- (33) Haddleton, D. M.; Kukulj, D.; Duncalf, D. J.; Heming, A. M.; Shooter, A. J. *Macromolecules* **1998**, *31*, 5201–5.
- (34) Haddleton, D. M.; Jasieczek, C. B.; Hannon, M. J.; Shooter, A. J. *Macromolecules* **1997**, *30*, 2190–3.
- (35) Small, B. L.; Brookhart, M. *Macromolecules* **1999**, *32*, 2120–30.
- (36) Small, B. L.; Brookhart, M. *J. Am. Chem. Soc.* **1998**, *120*, 7143–4.
- (37) Small, B. L.; Brookhart, M.; Bennett, A. M. A. *J. Am. Chem. Soc.* **1998**, *120*, 4049–50.
- (38) Haddleton, D. M.; Duncalf, D. J.; Kukulj, D.; Heming, A. M.; Shooter, A. J.; Clark, A. J. *J. Mater. Chem.* **1998**, *8*, 1525–32.
- (39) Sargeson, A. M.; Searle, G. H. *Inorg. Chem.* **1967**, *6*, 787.
- (40) *Comprehensive Coordination Chemistry*; Wilkinson, G., Ed.; Pergamon Press: Oxford, U.K., 1987; Vol. 2, Chapter 13.1, pp 50–6 and references therein.
- (41) Aldrich-Wright, J. R.; Vagg, R. S.; Williams, P. A. *Coord. Chem. Rev.* **1997**, *166*, 361–89.
- (42) Goodwin, H. A.; Lions, F. *J. Am. Chem. Soc.* **1960**, *82*, 5013–23.
- (43) Gibson, J. G.; McKenzie, E. D. *J. Chem. Soc. A* **1971**, 1666–83 and references therein.
- (44) Bosnich, B. *Proc. R. Soc. London Ser. A* **1967**, 88.
- (45) Bosnich, B.; Kneen, W. R. *Inorg. Chem.* **1970**, *9*, 2191–4.
- (46) Fenton, R. R.; Stephens, F. S.; Vagg, R. S.; Williams, P. A. *Inorg. Chim. Acta* **1992**, *201*, 157–64.
- (47) Fenton, R. R.; Stephens, F. S.; Vagg, R. S.; Williams, P. A. *Inorg. Chim. Acta* **1991**, *182*, 67–75.
- (48) Fenton, R. R.; Stephens, F. S.; Vagg, R. S.; Williams, P. A. *Inorg. Chim. Acta* **1992**, *197*, 233–42.
- (49) Michelsen, K.; Nielsen, K. M. *Acta Chem. Scand. A* **1980**, *34*, 755–64.
- (50) Glerup, J.; Goodson, P. A.; Hodgson, D. J.; Michelsen, K. *Inorg. Chem.* **1995**, *34*, 6255–64.
- (51) Glerup, J.; Michelsen, K.; Arulsamy, N.; Hodgson, D. J. *Inorg. Chim. Acta* **1998**, *274*, 155–166.
- (52) Hazell, R.; Jensen, K. B.; McKenzie, C. J.; Toftlund, H. *J. Chem. Soc., Dalton Trans.* **1995**, 707–17.

- (53) Glerup, J.; Goodson, P. A.; Hazell, A.; Hazell, R.; Hodgson, D. J.; McKenzie, C. J.; Michelsen, K.; Rychlewski, U.; Toftlund, H. *Inorg. Chem.* **1994**, *33*, 4105–11.
- (54) Branca, M.; Pispisa, B.; Aurisicchio, C. *J. Chem. Soc., Dalton Trans.* **1976**, 1543–6.
- (55) Melnyk, A. C.; Kjeldahl, N. K.; Redina, A. R.; Busch, D. H. *J. Am. Chem. Soc.* **1979**, *101*, 3232–40.
- (56) Cairns, C. J.; Heckman, R. A.; Melnyk, A. C.; Davis, W. M.; Busch, D. H. *J. Chem. Soc., Dalton Trans.* **1987**, 2505–10.
- (57) Leising, R. A.; Kim, J.; Perez, M. A.; Que, L., Jr. *J. Am. Chem. Soc.* **1993**, *115*, 9524–30.
- (58) Rabion, A.; Chen, S.; Wang, J.; Buchanan, R. M.; Seris, J.-L.; Fish, R. H. *J. Am. Chem. Soc.* **1995**, *117*, 12356–7.
- (59) Rieger, B.; Abu-Surrah, A. S.; Fawzi, R.; Steiman, M. *J. Organomet. Chem.* **1995**, *497*, 73–9.
- (60) For a discussion of this issue in relation to the trien ligand, refer to the following: Bosnich, B.; Gillard, R. D.; McKenzie, E. D.; Webb, G. A. *J. Chem. Soc. A* **1966**, 1331–9 and references therein.
- (61) Fenton, R. R.; Vagg, R. S.; Williams, P. A. *Inorg. Chim. Acta* **1988**, *148*, 37–44.
- (62) Chambers, J. A.; Mulqi, M. W.; Williams, P. A.; Vagg, R. S. *Inorg. Chim. Acta* **1984**, *81*, 55–60.
- (63) Chambers, J. A.; Goodwin, T. J.; Mulqi, M. W.; Williams, P. A.; Vagg, R. S. *Inorg. Chim. Acta* **1984**, *88*, 193–9.
- (64) Heinrichs, M. A.; Hodgson, D. J.; Michelsen, K.; Pedersen, E. *Inorg. Chem.* **1984**, *23*, 3174–80.
- (65) Bosnich, B.; Kneen, W. R.; Phillip, A. T. *Inorg. Chem.* **1969**, *8*, 2567–74.
- (66) Bernal, I.; Cetrullo, J.; Worrell, J. H.; Li, T. *Polyhedron* **1994**, *13*, 463–8.
- (67) Toscano, P. J.; Fordon, K. J.; Engelhardt, L. M.; Skelton, B. W.; White, A. H.; Marzilli, P. A. *Polyhedron* **1990**, *9*, 1079.
- (68) Dwyer, F. P.; Garvan, F. L. *J. Am. Chem. Soc.* **1959**, *81*, 2955–7.
- (69) Dwyer, F. P.; MacDermott, T. E. *J. Am. Chem. Soc.* **1963**, *85*, 2916–9.

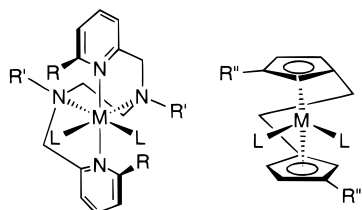
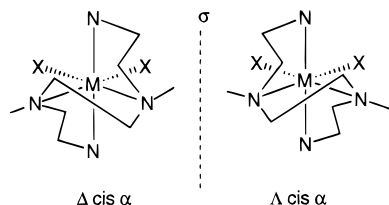


Figure 3. Comparison of cis  $\alpha$  and ansa metallocene complexes.

#### Achiral Ethylenediamine Backbone



#### Chiral S-Propylenediamine Backbone

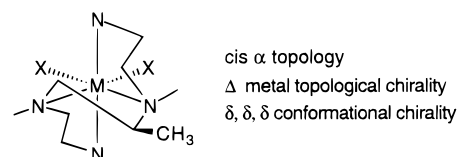
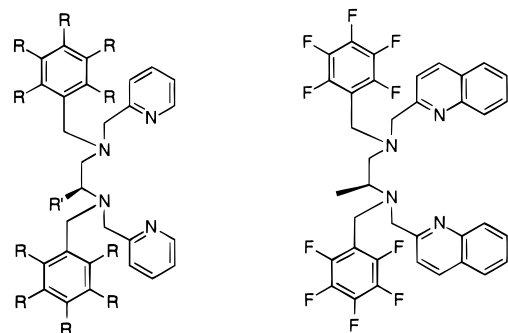


Figure 4. Topological and conformational chirality in quadridentate chelates.

donor group and the substituent on N (or lone pair on S) are oriented anti to each other in the cis  $\alpha$  arrangement.<sup>47</sup> It is interesting to compare cis  $\alpha$  complexes and ansa metallocenes,<sup>70–73</sup> which are similar in topology. They differ in that strapped metallocene ligands bind “face on” via cyclopentadienyl (Cp) and its analogues, with substituents projecting out and away from the reaction wedge for many derivatives. In contrast, the terminal donor groups on cis  $\alpha$  pyridylamine ligands bind “edge on” and R groups point more directly at substrate binding sites (Figure 3).

While these principles may be exploited to impose a nonplanar  $C_2$ -symmetric cis  $\alpha$  topology, other features must be incorporated to make the ligand stereoselective and, in some cases, even stereospecific.<sup>41</sup> In many chelating ligands, the introduction of one or more chiral centers on the internal chelate ring backbone has been sufficient to ensure that a single diastereomer is obtained. For example, when the sexadentate chelate *S*-propylenediamine tetraacetic acid (*S*-PDTA) binds to metal ions, the methyl substituent assumes a pseudoequatorial position on the puckered five-membered chelate ring. This preference fixes the conformational chirality of the metal propylenediamine ring as  $\delta$ , which in turn, controls the way in which the terminal donor groups wrap to give exclusively the  $\Delta$  absolute configuration about the metal center.<sup>68,69</sup> A similar kind of diastereoselection has been observed in amine-based quadridentate chelates prepared from enantiomerically pure chiral diamines (Figure 4).<sup>41</sup>

Taking these concepts and precedent with related systems into account, we have prepared a series of quadridentate ligands (Figure 5) and their first-row transition metal complexes. This study was undertaken as a prelude to screening these complexes



- 1 R, R' = H; en(Bn)py
- 2 R = F, R' = H; en(F<sub>5</sub>Bn)py
- 3 R = F, R' = CH<sub>3</sub>; S-pn(F<sub>5</sub>Bn)py

4 S-pn(F<sub>5</sub>Bn)qn

Figure 5. Quadridentate pyridylamine ligands.

as catalysts for a variety of reactions. The first goal was to identify convenient and versatile synthetic routes to ligand targets. Ethylenediamine (en) and the chiral *S*-propylenediamine (*S*-pn) were employed as the backbones for comparison.<sup>46,74</sup> Ligands based on the bulkier *R,R*-diaminocyclohexane and their complexation chemistry are the subject of a future report.<sup>75</sup> For the *S*-pn system, ligands with pyridyl, **3**, and quinolyl, **4**, donor groups were prepared to vary the steric bulk in the terminal donor positions of the quadridentate. To determine whether subtle differences in the electronic nature of substituents might influence physical properties, both  $-\text{CH}_2\text{C}_6\text{H}_5$ , **1**,<sup>76</sup> and  $-\text{CH}_2\text{C}_6\text{F}_5$ , **2**, analogues of the achiral en backbone ligand were synthesized. Benzyl groups were also chosen for their steric bulk and their potential to improve solubility in organic solvents. Since many reactions are promoted by Lewis acidic metal centers, electron withdrawing fluorine substituents were introduced to generate more electron deficient complexes. Moreover, since pyridine and quinoline groups are  $\pi$  acidic, these donors are also expected to enhance Lewis acidity. Depending upon the particular metal ion, the steric features of the ligand, and the donor strength of the counterions, six, five, or four coordinate structures could be obtained upon reaction of quadridentates with divalent metal halide salts,  $\text{MX}_2$ . Ultimately, complexes prepared from metal halides may be further activated to coordinate Lewis basic substrates by exchanging the halides for triflates,  $\text{OTf}^-$ , hexafluoroantimonates,  $\text{SbF}_6^-$ , hexafluorophosphates,  $\text{PF}_6^-$ , tetraphenylborates,  $\text{BPh}_4^-$ , or other weakly coordinating counterions via metathesis with the respective silver salts. The synthesis of these ligands and many of their first-row transition metal complexes, as well as structural and physical characterization, are discussed below.

## Experimental Section

**General Considerations.** All reagents and solvents were used as received from commercial sources (Aldrich, Acros, Strem) unless otherwise indicated. Pyridinecarboxaldehyde was distilled under vacuum prior to use. THF was dried and purified on alumina columns.<sup>77</sup> Cyclic voltammetric measurements were made either with a Bioanalytical Systems, Inc., model CV-27 or a Bioanalytical Systems model CV-

(70) Hoveyda, A. H.; Morken, J. P. *Angew. Chem., Int. Ed. Engl.* **1996**, *35*, 1263–84.

(71) Alt, H. G.; Samuel, E. *Chem. Soc. Rev.* **1998**, *27*, 323–9.

(72) Petasis, N. A.; Hu, Y. H. *Curr. Org. Chem.* **1997**, *1*, 249–86.

(73) Soga, K.; Shiono, T. *Prog. Polym. Sci.* **1997**, *22*, 1503–46.

(74) Goodwin, T. J.; Vagg, R. S.; Williams, P. A. *J. Proc. R. Soc. New South Wales* **1984**, *117*, 1–6.

(75) Ng, C.; Savage, S. A.; Derringer, D.; Sabat, M.; Campana, C.; Fraser, C. L. Manuscript in preparation.

(76) Reference to the prior synthesis of en(Bn)py appeared in the course of our work with this ligand, **1**.<sup>41</sup> Aldrich-Wright, J. R. Ph.D. Thesis, Macquarie University, 1993.

(77) Pangborn, A. B.; Giardello, M. A.; Grubbs, R. H.; Rosen, R. K.; Timmers, F. J. *Organometallics* **1996**, *15*, 1518–20.

50W instrument on dichloromethane solutions that contained 0.1 M tetra-*n*-butylammonium hexafluorophosphate (TBAH) as the supporting electrolyte. A glassy carbon electrode and a Pt-wire electrode were utilized.  $E_{1/2}$  values, determined as  $(E_{p,a} + E_{p,c})/2$ , were referenced to the aqueous Ag/AgCl electrode at room temperature and are uncorrected for junction potentials. Under our experimental conditions the ferrocenium/ferrocene couple is at  $E_{1/2} = 0.47$  V vs Ag/AgCl. Voltammograms shown in Figure 8 were referenced vs a nonaqueous ( $\text{CH}_3\text{CN}$ ) Ag/AgCl electrode. Under these conditions the ferrocene couple is observed at  $E_{1/2} = 0.24$  V. Conductivity measurements were performed at room temperature on 1 mM acetonitrile solutions using a YSI model 35 conductance meter. Infrared spectra were recorded as mineral oil (Nujol) mulls supported on NaCl plates in the region  $4000\text{--}600\text{ cm}^{-1}$  using a Nicolet Impact 400 Fourier transform spectrometer. Electronic absorption spectra were recorded on Hewlett-Packard diode array spectrophotometers, either model HP8452A (200–800 nm) or model HP8453 (200–1100 nm).  $^1\text{H}$  and  $^{13}\text{C}$  NMR spectra were recorded at 300 and 75 MHz, respectively, on either a GE QE-300 or a GN-300 spectrometer. Elemental microanalyses were performed on a Perkin-Elmer model 2400 Series II CHNS/O analyzer or were determined by Atlantic Microlab, Inc., Norcross, GA.

**Ligand Syntheses. 1,6-Diphenyl-2,5-bis(2-methylpyridyl)-2,5-diazahexane, en(Bn)py (1).** Ethylenediamine (2.1 mL, 0.031 mol) was stirred with 2-pyridinecarboxaldehyde (6 mL, 0.063 mol) in  $\text{CH}_2\text{Cl}_2$  (40 mL) containing molecular sieves for 2 h. The reaction was then filtered and concentrated to give the Schiff base as a pale yellow oil: 7.10 g, 95%.<sup>78,79</sup> The diimine (7.10 g, 0.030 mol) was dissolved in MeOH (50 mL),  $\text{NaBH}_4$  (2.48 g, 0.066 mol) was added, and the reaction was stirred for 30 min at room temperature. Aqueous HCl (3 M, 24 mL) was added slowly with stirring, and then the MeOH was removed via rotary evaporation. Aqueous NaOH (20%) was added until the solution reached pH > 10. The product was extracted with  $\text{CH}_2\text{Cl}_2$  ( $4 \times 50$  mL), was washed with  $\text{H}_2\text{O}$  ( $2 \times 50$  mL) and brine (50 mL), and then was dried over  $\text{Na}_2\text{SO}_4$ . Following filtration and concentration, the diamine was obtained as a yellow oil: 6.0 g, 83%.<sup>42,80</sup> Alkylation was effected by dissolving the diamine (0.742 g, 3.06 mmol) in dry THF (50 mL) and deprotonating with NaH (0.476 g, 19.8 mmol). The mixture was cooled to 0 °C and was stirred for ~20 min prior to addition of benzyl bromide (1.1 mL, 9.3 mmol). The reaction was allowed to warm to room temperature slowly and then was stirred at that temperature for an additional 12 h. Water (15 mL) and then HCl (3 M) were added until the solution reached pH = 2. The acidic mixture was concentrated in vacuo to remove THF and then was washed with  $\text{Et}_2\text{O}$  ( $3 \times 20$  mL). The aqueous solution was made basic (pH > 10) through addition of NaOH (10%), was saturated with NaCl, and then was extracted with  $\text{EtOAc}$  ( $4 \times 20$  mL). The solution was dried over  $\text{Na}_2\text{SO}_4$ , filtered, and concentrated to yield the product, **1**, as an off-white solid: 1.22 g, 80%. The ligand may be further purified by silica gel flash chromatography with  $\text{EtOAc}$ .  $^1\text{H}$  NMR ( $\text{CDCl}_3$ , 300 MHz):  $\delta$  2.68 (s, 4H), 3.57 (s, 4H), 3.70 (s, 4H), 7.11 (m, 2H), 7.25 (m, 10H), 7.45 (d,  $J = 8.1$  Hz, 2H), 7.57 (m, 2H), 8.48 (d,  $J = 5.0$ , 2H).

**1,6-Bis(pentafluorophenyl)-2,5-bis(2-methylpyridyl)-2,5-diazahexane, en(F<sub>5</sub>Bn)py (2).** The ligand **2** was prepared by the method described for **1** using  $\alpha$ -bromo-2,3,4,5,6-pentafluorotoluene instead of benzyl bromide. In the final work up, after the aqueous layer was made basic, the alkylated product was extracted with  $\text{CH}_2\text{Cl}_2$  instead of  $\text{EtOAc}$ . The ligand, **2**, was obtained as a white crystalline solid: 2.44 g, 87%.  $^1\text{H}$  NMR ( $\text{CDCl}_3$ , 300 MHz):  $\delta$  2.66 (s, 4H), 3.74 (s, 4H), 3.76 (s, 4H), 7.14 (m, 2H), 7.34 (d,  $J = 7.9$  Hz, 2H), 7.60 (m, 2H), 8.48 (d,  $J = 4.3$  Hz, 2H).

**3S-Methyl-1,6-bis(pentafluorophenyl)-2,5-bis(2-methylpyridyl)-2,5-diazahexane, S-pn(F<sub>5</sub>Bn)py (3).** L-Alanine methyl ester hydrochloride was converted to the free base by passing a MeOH solution

(400 mL) of the HCl salt (21.33 g, 0.153 mol) through a column of strongly basic Amberlite 402 anion-exchange resin (225 g, 17% capacity): 10.84 g. Yield: 69% by NMR integrations. The resulting ester was reacted with  $\text{NH}_3$  in a saturated MeOH solution to form the amide, which was subsequently reduced with  $\text{BH}_3 \cdot \text{THF}$  and worked up as described by Miller et al.<sup>82</sup> to produce *S*-propylenediamine as its HCl salt. *S*-propylenediamine·2HCl (0.980 g, 6.66 mmol) was crushed into a powder and then was suspended in  $\text{CH}_3\text{CN}$  (50 mL). Triethylamine (18 mL, 0.13 mol) and 2-pyridinecarboxaldehyde (1.3 mL, 0.014 mol) were added, and the reaction was allowed to stir for ~15 h at 25 °C. After this time,  $\text{H}_2\text{O}$  (30 mL) was added and the aqueous layer was extracted with  $\text{CH}_2\text{Cl}_2$  ( $5 \times 50$  mL). Combined  $\text{CH}_2\text{Cl}_2$  layers were dried over  $\text{Na}_2\text{SO}_4$ , filtered, and concentrated in vacuo to give the crude Schiff base product as a yellow orange oil: 1.50 g, 89%.  $^1\text{H}$  NMR ( $\text{CDCl}_3$ , 300 MHz):  $\delta$  1.39 (d,  $J = 6.1$  Hz, 3H), 3.89 (m, 3H), 7.28 (m, 2H), 7.70 (m, 2H), 7.97 (m, 2H), 8.36 (s, 1H), 8.40 (s, 1H), 8.61 (m, 2H). The resulting diimine was reduced with  $\text{NaBH}_4$  in MeOH by the general procedure described above for **1**: 1.14 g, 75%.<sup>83</sup>  $^1\text{H}$  NMR ( $\text{CDCl}_3$ , 300 MHz):  $\delta$  1.11 (d,  $J = 6.1$  Hz, 3H), 2.71–2.56 (br m, 2H), 2.84 (m, 1H), 4.01–3.83 (br m, 4H), 7.14 (m, 2H), 7.33 (d,  $J = 7.3$  Hz, 2H), 7.62 (m, 2H), 8.49 (d,  $J = 4.9$  Hz, 2H). Alkylation of the resulting diamine was effected by the method described for **1** using  $\alpha$ -bromo-2,3,4,5,6-pentafluorotoluene in place of benzyl bromide. In the final workup, after the aqueous layer was made basic, the alkylated product was extracted with  $\text{Et}_2\text{O}$  instead of  $\text{EtOAc}$ . The crude ligand, **3**, was obtained as a viscous brown oil which solidified upon standing: 2.37 g, 87%. Typically the crude ligand **3** was not purified prior to reaction with metal chloride salts. However further purification may be effected by dissolving the crude ligand in  $\text{Et}_2\text{O}$  and adding hexanes to precipitate a viscous brown impurity. After filtration through Celite and concentration, the resulting residue may be recrystallized from  $\text{Et}_2\text{O}$ /hexanes to yield **3** as a beige powder.  $^1\text{H}$  NMR ( $\text{CDCl}_3$ , 300 MHz):  $\delta$  1.07 (d,  $J = 6.6$  Hz, 3H), 2.43 (m, 1H), 2.73 (m, 1H), 2.98 (q,  $J = 6.6$  Hz, 1H), 3.70 (m, 8H), 7.11 (m, 2H), 7.39 (d,  $J = 7.8$  Hz, 2H), 7.59 (m, 2H), 8.42 (d,  $J = 4.2$  Hz, 1H), 8.47 (d,  $J = 5.1$  Hz, 1H).

**3S-Methyl-1,6-bis(pentafluorophenyl)-2,5-bis(2-methylquinolyl)-2,5-diazahexane, S-pn(F<sub>5</sub>Bn)qn (4).** Crushed *S*-pn·2HCl was suspended in  $\text{CH}_3\text{CN}$  (54 mL), and then  $\text{Et}_3\text{N}$  (18 mL) and 2-quinoline carboxaldehyde (2.22 g, 14.0 mmol) were added. The reaction was stirred for 15 h at 25 °C.  $\text{H}_2\text{O}$  (20 mL) was added, and the solution was extracted with  $\text{CH}_2\text{Cl}_2$  ( $4 \times 40$  mL). Combined organic layers were washed with  $\text{H}_2\text{O}$  ( $2 \times 40$  mL) and with saturated brine ( $2 \times 40$  mL) and then were dried over  $\text{Na}_2\text{SO}_4$ . After filtration and concentration via rotovap, the crude Schiff base product was obtained as a brownish solid. The crude solid was dissolved in a minimal amount of  $\text{CH}_2\text{Cl}_2$ , and hexanes were added until a dark brown residue precipitated. The remaining supernatant was filtered through Celite and then was concentrated in vacuo just to the point when crystallization commenced. After being chilled at 0 °C for 2 h, the pale yellow crystalline solid was collected by filtration, was washed with a minimal amount of hexanes, and then was dried in vacuo: 1.48 g, 62%.  $^1\text{H}$  NMR ( $\text{CDCl}_3$ , 300 MHz):  $\delta$  1.45 (d,  $J = 5.5$  Hz, 3H), 4.00 (m, 3H), 7.55 (m, 2H), 7.72 (m, 2H), 7.82 (d,  $J = 7.9$  Hz, 2H), 8.08 (s, 1H), 8.11 (s, 1H), 8.16 (m, 4H), 8.57 (s, 1H), 8.61 (s, 1H). The diimine was reduced with  $\text{NaBH}_4$  in MeOH by the general procedure described for **1** to give the crude diamine as a tan oil in essentially quantitative yield.  $^1\text{H}$  NMR ( $\text{CDCl}_3$ , 300 MHz):  $\delta$  1.17 (d,  $J = 6.1$  Hz, 3H), 3.02–2.68 (br m, 3H), 4.24–4.05 (br m, 4H), 7.52–7.47 (m, 4H), 7.66 (m, 2H), 7.77 (d,  $J = 8.6$  Hz, 2H), 8.02 (d,  $J = 3.6$  Hz, 2H), 8.09 (d,  $J = 3.6$  Hz, 2H). The diamine was subsequently alkylated with  $\alpha$ -bromo-2,3,4,5,6-pentafluorotoluene in THF in the presence of NaH by the standard procedure described for **1**. In the final workup, after the aqueous layer was made basic, the alkylated product was extracted with  $\text{Et}_2\text{O}$  instead of  $\text{EtOAc}$ . The product, **4**, was obtained as a brittle yellow solid: 2.19

(78) For other preparations of the diimine see: DeVos, D. E.; Feijen, E. J. P.; Schoonheydt, R. A.; Jacobs, P. A. *J. Am. Chem. Soc.* **1994**, *116*, 4746–52.

(79) Busch, D. H.; Bailer, J. C., Jr. *J. Am. Chem. Soc.* **1956**, *78*, 1137.

(80) For previous preparations and uses of this pyridyldiamine see ref 43 and: Newkome, G. R.; Frere, Y. A.; Fronczek, F. R.; Gupta, V. K. *Inorg. Chem.* **1985**, *24*, 1001–6.

(81) Basak, A. K.; Martell, A. E. *Inorg. Chem.* **1988**, *27*, 1948–55.

(82) Miller, D. D.; Hsu, F.-L.; Ruffolo, R. R., Jr.; Patil, P. N. *J. Med. Chem.* **1976**, *19*, 1382–4.

(83) For another preparation of  $\beta$ -pnHpy diamine see ref 49 and the following: McCollum, D. G.; Fraser, C.; Ostrander, R.; Rheingold, A. L.; Bosnich, B. *Inorg. Chem.* **1994**, *33*, 2383–92.

g, 77%.  $^1\text{H}$  NMR ( $\text{CDCl}_3$ , 300 MHz):  $\delta$  1.12 (d,  $J = 6.9$  Hz, 3H), 2.51 (m, 1H), 2.84 (m, 1H), 3.08 (m, 1H), 3.78 (m, 8H), 7.49 (m, 4H), 7.68 (m, 2H), 7.76 (m, 2H), 7.99 (m, 4H).

**Preparation of Metal Complexes.** Metal complexes were prepared by reaction of alcohol (EtOH or MeOH) solutions of the appropriate metal chloride salt with an alcohol solution of the ligand. A typical reaction scale is as follows: ligand (0.15 mmol); metal chloride salt (0.16 mmol); alcohol (3 mL total). For the less soluble ligands, **2** and **4**, a minimal amount of methylene chloride was sometimes added to facilitate dissolution. In cases where the complexes precipitated from the reaction solution, they were collected by filtration. Otherwise the solutions were concentrated in vacuo and the residues were purified by recrystallization. Specific purification procedures and deviations from this standard method are indicated below for the respective compounds.

**Metal Complexes of en(Bn)py (1).**  $[\text{Mn}\{\text{en}(\text{Bn})\text{py}\}\text{Cl}_2] \cdot 0.5\text{CH}_2\text{Cl}_2$ . The reaction solution was concentrated in vacuo. The resulting residue was recrystallized from  $\text{CH}_2\text{Cl}_2/\text{Et}_2\text{O}$  to give the Mn(II) complex as a white microcrystalline solid. Yield: 74%.  $\Lambda_{\text{M}} = 0.20 \Omega^{-1} \text{ mol}^{-1} \text{ cm}^2$ . Anal. Calcd for  $\text{C}_{28.5}\text{H}_{31}\text{N}_4\text{Cl}_3\text{Mn}$ : C, 57.93; H, 5.29; N, 9.48. Found: C, 57.61; H, 5.68; N, 9.30.

**$[\text{Fe}\{\text{en}(\text{Bn})\text{py}\}\text{Cl}_2] \cdot 0.5\text{CH}_2\text{Cl}_2$ .** The  $\text{CH}_2\text{Cl}_2/\text{EtOH}$  reaction mixture was concentrated in vacuo. The resultant yellow residue was recrystallized from  $\text{CH}_2\text{Cl}_2/\text{hexanes}$  to give canary yellow needles. Yield: 82%.  $\Lambda_{\text{M}} = 0.13 \Omega^{-1} \text{ mol}^{-1} \text{ cm}^2$ . Anal. Calcd for  $\text{C}_{28.5}\text{H}_{31}\text{N}_4\text{Cl}_3\text{Fe}$ : C, 57.84; H, 5.28; N, 9.47. Found: C, 58.23; H, 5.44; N, 9.43.

**$[\text{Co}\{\text{en}(\text{Bn})\text{py}\}\text{Cl}_2] \cdot 0.5\text{CH}_2\text{Cl}_2$ .** The Co(II) compound was recrystallized by vapor diffusion of  $\text{Et}_2\text{O}$  into a  $\text{CH}_2\text{Cl}_2/\text{Et}_2\text{O}$  solution of the complex to yield a purple microcrystalline solid. Yield: 85%.  $\Lambda_{\text{M}} = 5.6 \Omega^{-1} \text{ mol}^{-1} \text{ cm}^2$ . Anal. Calcd for  $\text{C}_{28.5}\text{H}_{31}\text{N}_4\text{Cl}_3\text{Co}$ : C, 57.54; H, 5.25; N, 9.42. Found: C, 57.14; H, 5.60; N, 9.32.

**$[\text{Zn}\{\text{en}(\text{Bn})\text{py}\}\text{Cl}_2]$ .** The Zn(II) compound was recrystallized by vapor diffusion of  $\text{Et}_2\text{O}$  into a  $\text{CH}_2\text{Cl}_2/\text{Et}_2\text{O}$  solution to yield a pale yellow microcrystalline solid. Yield: 66%.  $\Lambda_{\text{M}} = 1.7 \Omega^{-1} \text{ mol}^{-1} \text{ cm}^2$ .  $^1\text{H}$  NMR ( $\text{CDCl}_3$ , 300 MHz):  $\delta$  2.34, 2.57 (system AB,  $J_{\text{AB}} = 4.4$  Hz, 4H), 3.18, 4.96 (system AB,  $J_{\text{AB}} = 14.4$  Hz, 4H), 3.42, 4.64 (system AB,  $J_{\text{AB}} = 13.7$ , 4H), 7.12 (br s, 4H), 7.22 (d,  $J = 6.39$ , 2H), 7.35 (m, 6H), 7.41 (t, 2H), 7.81 (t, 2H), 9.73 (s, 2H).  $^{13}\text{C}$  NMR ( $\text{CDCl}_3$ , 75 MHz):  $\delta$  43.8, 54.4, 58.3, 123.3, 123.6, 127.9, 128.1, 131.0, 131.9, 138.5, 149.6, 154.1.

**Metal Complexes of en(F<sub>5</sub>Bn)py (2).**  $[\text{Mn}\{\text{en}(\text{F}_5\text{Bn})\text{py}\}\text{Cl}_2] \cdot 0.5\text{CH}_3\text{CH}_2\text{OH}$ . The Mn(II) complex was prepared from  $\text{MnCl}_2$  and the tetra-HCl salt of the ligand, **2**, in EtOH solution. White needles precipitated from the EtOH solution. Yield: 97%.  $\Lambda_{\text{M}} = 1.4 \Omega^{-1} \text{ mol}^{-1} \text{ cm}^2$ . Anal. Calcd for  $\text{C}_{29}\text{H}_{33}\text{N}_4\text{O}_{0.5}\text{F}_{10}\text{Cl}_2\text{Mn}$ : C, 46.36; H, 3.09; N, 7.46. Found: C, 46.27; H, 3.04; N, 7.26.

**$[\text{Fe}\{\text{en}(\text{F}_5\text{Bn})\text{py}\}\text{Cl}_2]\text{PF}_6$ .** The Fe(III) complex precipitated from EtOH solution upon addition of excess  $\text{NH}_4\text{PF}_6$  (3 equiv). The resulting yellow residue was recrystallized from  $\text{CH}_3\text{CN}/\text{EtOH}$  to yield a canary yellow microcrystalline solid. Yield: 62%.  $\Lambda_{\text{M}} = 97 \Omega^{-1} \text{ mol}^{-1} \text{ cm}^2$ . Anal. Calcd for  $\text{C}_{28}\text{H}_{20}\text{N}_4\text{PF}_6\text{Cl}_2\text{Fe}$ : C, 38.50; H, 2.31; N, 6.41. Found: C, 38.42; H, 2.46; N, 6.16.

**$[\text{Fe}\{\text{en}(\text{F}_5\text{Bn})\text{py}\}\text{Cl}_2] \cdot \text{CH}_2\text{Cl}_2$ .** The EtOH reaction mixture was concentrated in vacuo, and the resulting crude Fe(II) compound was recrystallized from  $\text{CH}_2\text{Cl}_2/\text{hexanes}$  to give powdery canary yellow needles. Yield: 92%.  $\Lambda_{\text{M}} = 0.8 \Omega^{-1} \text{ mol}^{-1} \text{ cm}^2$ . Anal. Calcd for  $\text{C}_{29}\text{H}_{22}\text{N}_4\text{F}_{10}\text{Cl}_4\text{Fe}$ : C, 42.78; H, 2.72; N, 6.88. Found: C, 42.45; H, 2.92; N, 6.65.

**$[\text{Co}\{\text{en}(\text{F}_5\text{Bn})\text{py}\}\text{Cl}_2] \cdot 0.5\text{CH}_3\text{CH}_2\text{OH} \cdot 0.5\text{CH}_2\text{Cl}_2$ .** The Co(II) complex was obtained as lavender needles by concentration of the EtOH reaction mixture, followed by recrystallization of the resulting residue by evaporation of  $\text{CH}_2\text{Cl}_2$  from a  $\text{CH}_2\text{Cl}_2/\text{EtOH}$  solution. Yield: 90%.  $\Lambda_{\text{M}} = 7.6 \Omega^{-1} \text{ mol}^{-1} \text{ cm}^2$ . Anal. Calcd for  $\text{C}_{29.5}\text{H}_{24}\text{N}_4\text{O}_{0.5}\text{F}_{10}\text{Cl}_3\text{Co}$ : C, 44.10; H, 3.03; N, 7.02. Found: C, 44.33; H, 3.00; N, 7.03. (Note: The  $^1\text{H}$  NMR spectrum obtained after oxidation of this complex to Co(III) confirms the presence of these associated solvents. This spectrum is provided as part of the Supporting Information.)

**$[\text{Ni}\{\text{en}(\text{F}_5\text{Bn})\text{py}\}\text{Cl}_2] \cdot 0.5\text{CH}_3\text{CH}_2\text{OH}$ .** The Ni(II) complex was prepared from  $\text{NiCl}_2$  and the tetra-HCl salt of the ligand. It precipitated as mint green needles from the EtOH reaction medium. Yield: 79%.  $\Lambda_{\text{M}} = 22 \Omega^{-1} \text{ mol}^{-1} \text{ cm}^2$ . Anal. Calcd for  $\text{C}_{29}\text{H}_{23}\text{N}_4\text{O}_0.5\text{F}_{10}\text{Cl}_2\text{Ni}$ : C, 45.76; H, 2.96; N, 7.49. Found: C, 46.05; H, 2.79; N, 7.48.

**$[\text{Cu}\{\text{en}(\text{F}_5\text{Bn})\text{py}\}\text{Cl}_2] \cdot 0.5\text{CH}_3\text{OH}$ .** The Cu(II) compound was obtained as a mint green microcrystalline solid after slow evaporation of  $\text{CH}_2\text{Cl}_2$  from a  $\text{CH}_2\text{Cl}_2/\text{MeOH}$  solution of the complex. Yield: 93%.  $\Lambda_{\text{M}} = 54 \Omega^{-1} \text{ mol}^{-1} \text{ cm}^2$ . Anal. Calcd for  $\text{C}_{28.5}\text{H}_{22}\text{N}_4\text{O}_{0.5}\text{F}_{10}\text{Cl}_2\text{Cu}$ : C, 45.46; H, 2.95; N, 7.44. Found: C, 45.54; H, 2.99; N, 7.13.

**$[\text{Zn}\{\text{en}(\text{F}_5\text{Bn})\text{py}\}\text{Cl}_2] \cdot \text{CH}_3\text{OH}$ .** This complex was obtained as white needles. Yield: 84%.  $\Lambda_{\text{M}} = 5.1 \Omega^{-1} \text{ mol}^{-1} \text{ cm}^2$ . Anal. Calcd for  $\text{C}_{29}\text{H}_{24}\text{N}_4\text{OF}_{10}\text{Cl}_2\text{Zn}$ : C, 45.14; H, 3.14; N, 7.27. Found: C, 45.42; H, 3.01; N, 7.14.  $^1\text{H}$  NMR ( $\text{CDCl}_3$ , 300 MHz):  $\delta$  2.23, 2.49 (system AB,  $J_{\text{AB}} = 11$  Hz, 4H), 3.36 (d,  $J = 15.4$  Hz, 2H), 3.48 (m, 2H), 4.83 (d,  $J = 14.6$  Hz, 2H), 5.05 (d,  $J = 14.3$  Hz, 2H), 7.30 (d,  $J = 7.7$  Hz, 2H), 7.47 (t, 2H), 7.87 (t, 2H), 9.75 (d,  $J = 4.6$  Hz, 2H).  $^{13}\text{C}$  NMR ( $\text{CDCl}_3$ , 75 MHz):  $\delta$  42.4, 45.5, 57.3, 123.7, 124.0, 135.4, 139.2, 142.6, 143.6, 147.0, 149.5, 153.6.

**Metal complexes of S-pn(F<sub>5</sub>Bn)py (3).**  $[\text{Mn}\{\text{S-pn}(\text{F}_5\text{Bn})\text{py}\}\text{Cl}_2]$ . The Mn(II) complex precipitated from the EtOH reaction solution as a white microcrystalline solid. Yield: 85%.  $\Lambda_{\text{M}} = 2.0 \Omega^{-1} \text{ mol}^{-1} \text{ cm}^2$ . Anal. Calcd for  $\text{C}_{29}\text{H}_{22}\text{N}_4\text{F}_{10}\text{Cl}_2\text{Mn}$ : C, 46.92; H, 2.99; N, 7.55. Found: C, 46.69; H, 3.28; N, 7.35.

**$[\text{Fe}\{\text{S-pn}(\text{F}_5\text{Bn})\text{py}\}\text{Cl}_2] \cdot 0.5\text{CH}_2\text{Cl}_2$ .** The EtOH reaction mixture was concentrated in vacuo. The resulting residue was dissolved in  $\text{CH}_2\text{Cl}_2$  and precipitated from hexanes to produce a canary yellow powdery solid. Yield: 78%.  $\Lambda_{\text{M}} = 0.5 \Omega^{-1} \text{ mol}^{-1} \text{ cm}^2$ . Anal. Calcd for  $\text{C}_{29.5}\text{H}_{23}\text{N}_4\text{F}_{10}\text{Cl}_3\text{Fe}$ : C, 45.10; H, 2.95; N, 7.13. Found: C, 45.17; H, 3.26; N, 7.14.

**$[\text{Co}\{\text{S-pn}(\text{F}_5\text{Bn})\text{py}\}\text{Cl}_2]$ .** The Co(II) complex precipitated from the EtOH reaction solution as a lavender microcrystalline solid. Yield: 82%.  $\Lambda_{\text{M}} = 7.0 \Omega^{-1} \text{ mol}^{-1} \text{ cm}^2$ . Anal. Calcd for  $\text{C}_{29}\text{H}_{22}\text{N}_4\text{F}_{10}\text{Cl}_2\text{Co}$ : C, 46.67; H, 2.97; N, 7.51. Found: C, 46.28; H, 3.33; N, 7.16.

**$[\text{Ni}\{\text{S-pn}(\text{F}_5\text{Bn})\text{py}\}\text{Cl}_2]$ .** The Ni(II) complex precipitated from the EtOH reaction solution as a mint green microcrystalline solid. Yield: 34%.  $\Lambda_{\text{M}} = 30 \Omega^{-1} \text{ mol}^{-1} \text{ cm}^2$ . Anal. Calcd for  $\text{C}_{29}\text{H}_{22}\text{N}_4\text{F}_{10}\text{Cl}_2\text{Ni}$ : C, 46.69; H, 2.97; N, 7.51. Found: C, 46.53; H, 3.31; N, 7.33.

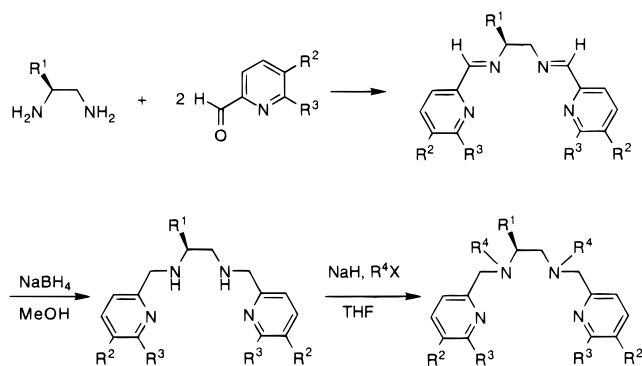
**$[\text{Cu}\{\text{S-pn}(\text{F}_5\text{Bn})\text{py}\}\text{Cl}_2] \cdot 0.5\text{CH}_2\text{Cl}_2$ .** The Cu(II) compound precipitated as a lime green powder from a  $\text{CH}_2\text{Cl}_2/\text{Et}_2\text{O}$  solution. Yield: 71%.  $\Lambda_{\text{M}} = 92 \Omega^{-1} \text{ mol}^{-1} \text{ cm}^2$ . Anal. Calcd for  $\text{C}_{29.5}\text{H}_{23}\text{N}_4\text{F}_{10}\text{Cl}_3\text{Cu}$ : C, 44.66; H, 2.92; N, 7.06. Found: C, 44.54; H, 3.27; N, 7.30.

**$[\text{Zn}\{\text{S-pn}(\text{F}_5\text{Bn})\text{py}\}\text{Cl}_2]$ .** The Zn(II) complex precipitated from the EtOH reaction solution as a white microcrystalline solid. Yield: 67%.  $\Lambda_{\text{M}} = 36 \Omega^{-1} \text{ mol}^{-1} \text{ cm}^2$ . Anal. Calcd for  $\text{C}_{29}\text{H}_{22}\text{N}_4\text{F}_{10}\text{Cl}_2\text{Zn}$ : C, 46.27; H, 2.95; N, 7.44. Found: 46.13; H, 3.24; N, 7.24. Major isomer:  $^1\text{H}$  NMR ( $\text{CDCl}_3$ , 300 MHz)  $\delta$  0.66 (d,  $J = 7.3$  Hz, 3 H), 2.12 (d,  $J = 11.6$  Hz, 1H), 2.47 (m, 1H), 2.87 (m, 1H), 3.34 (d,  $J = 6.1$  Hz, 1H), 3.39 (d,  $J = 5.5$  Hz, 1H), 3.45 (d,  $J = 14.0$  Hz, 1H), 4.05 (d,  $J = 14.0$ , 1H), 4.76 (d,  $J = 16.5$  Hz, 1H), 4.98 (m, 2H), 5.21 (d,  $J = 14.0$  Hz, 1H), 7.30 (d,  $J = 7.9$  Hz, 1H), 7.37 (d,  $J = 7.3$  Hz, 1H), 7.46 (m, 2H), 7.89 (m, 2H), 9.72 (m, 2H);  $^{13}\text{C}$  NMR ( $\text{CDCl}_3$ , 75 MHz)  $\delta$  11.7, 39.5, 43.0, 50.8, 51.3, 55.8, 57.2, 123.6, 123.8, 124.1, 139.1, 149.6, 149.7, 153.4, 154.4.

**Metal Complexes of S-pn(F<sub>5</sub>Bn)qn (4).**  $[\text{Co}\{\text{S-pn}(\text{F}_5\text{Bn})\text{qn}\}\text{Cl}_2] \cdot 0.5\text{CH}_2\text{Cl}_2$ . The Co(II) complex was obtained as a periwinkle microcrystalline solid after precipitation from  $\text{CH}_2\text{Cl}_2/\text{Et}_2\text{O}$ . Yield: 70%.  $\Lambda_{\text{M}} = 43 \Omega^{-1} \text{ mol}^{-1} \text{ cm}^2$ . Anal. Calcd for  $\text{C}_{37.5}\text{H}_{27}\text{N}_4\text{F}_{10}\text{Cl}_3\text{Co}$ : C, 50.67; H, 3.06; N, 6.30. Found: C, 50.78; H, 3.45; N, 6.23.

**$[\text{Zn}\{\text{S-pn}(\text{F}_5\text{Bn})\text{qn}\}\text{Cl}_2]$ .** The Zn(II) compound was obtained as a beige solid upon concentration of the EtOH/ $\text{CH}_2\text{Cl}_2$  solution. Yield: 46%.  $\Lambda_{\text{M}} = 29 \Omega^{-1} \text{ mol}^{-1} \text{ cm}^2$ . Major isomer:  $^1\text{H}$  NMR ( $\text{CDCl}_3$ , 300 MHz)  $\delta$  1.09 (d,  $J = 5.5$  Hz, 3H), 2.99 (d,  $J = 15.3$  Hz, 1H), 3.65 (m, 1H), 3.87 (m, 1H), 4.00 (d,  $J = 19.5$  Hz, 1H), 4.09 (d,  $J = 15.9$  Hz, 1H), 4.26 (d,  $J = 9.16$  Hz, 1H), 4.32 (d,  $J = 12.8$  Hz, 1H), 4.54 (d,  $J = 15.3$  Hz, 1H), 4.79 (d,  $J = 15.3$  Hz, 1H), 5.22 (m, 2H), 6.96 (m, 1H), 7.31 (m, 2H), 7.73 (m, 4H), 7.90 (d,  $J = 7.9$  Hz, 1H), 8.03 (m, 1H), 8.25 (d,  $J = 7.9$  Hz, 1H), 8.34 (d,  $J = 7.9$  Hz, 1H), 9.69 (d,  $J = 6.7$  Hz, 1H);  $^{13}\text{C}$  NMR ( $\text{CDCl}_3$ , 75 MHz)  $\delta$  13.2, 42.4, 46.2, 49.8, 55.8, 56.2, 59.6, 104.6, 108.8, 121.2, 122.7, 126.2, 127.0, 127.3, 128.0, 128.3, 129.7, 130.3, 135.6, 138.9, 139.6, 139.9, 140.9, 143.6, 144.0, 145.3, 147.2, 157.6, 159.7.

**Oxidation of Co(II) Complexes.** Co(II) complexes were oxidized with  $\text{H}_2\text{O}_2$  according to the procedure described by Fenton et al.<sup>46</sup> Oxidations with  $\text{Br}_2$  were performed by the procedure described below for  $[\text{Co}\{\text{en}(\text{Bn})\text{py}\}\text{Cl}_2]$ , and then  $^1\text{H}$  NMR spectra were recorded. If

**Scheme 1.** Quadridentate Ligand Synthesis

necessary, the solutions were warmed to dissolve the complexes prior to addition of bromine. Chemical shifts attributable to the major isomers evident in the  $^1\text{H}$  NMR spectra of the bromine reactions are tabulated below. Note: In all cases, minor products characterized by resonances at  $\sim 9.88\text{--}9.95$  ppm are present. It is estimated that these comprise up to 15–20% of the reaction mixture as determined by integration.

**[Co{en(Bn)py}Cl<sub>2</sub>] Oxidation.** [Co{en(Bn)py}Cl<sub>2</sub>] (8.7 mg, 0.015 mmol) and CDCl<sub>3</sub> (0.6 mL) were combined in an NMR tube. Bromine (0.050 mL, 0.97 mmol) was added, and a  $^1\text{H}$  NMR spectrum of the resultant red-brown solution was recorded.  $^1\text{H}$  NMR (CDCl<sub>3</sub>, 300 MHz):  $\delta$  2.85 (s, 4H), 3.35 (m, 4H), 4.48 (m, 2H), 5.13 (m, 2H), 7.34 (m, 4H), 7.55 (m, 6H), 7.62 (m, 2H), 7.72 (m, 2H), 8.09 (m, 2H), 9.64 (d,  $J = 5.8$  Hz, 2H).

**[Co{en(F<sub>5</sub>Bn)py}Cl<sub>2</sub>] Oxidation.**  $^1\text{H}$  NMR (CDCl<sub>3</sub>, 300 MHz):  $\delta$  2.97 (s, 4H), 3.42 (d,  $J = 14.2$  Hz, 2H), 3.93 (d,  $J = 15.0$  Hz, 2H), 4.72 (d,  $J = 15.4$  Hz, 2H), 5.21 (d,  $J = 15.4$  Hz, 2H), 7.76 (m, 4H), 8.17 (m, 2H), 9.68 (d,  $J = 5.8$  Hz, 2H). This spectrum is provided as part of the Supporting Information.

**[Co{S-pn(F<sub>5</sub>Bn)py}Cl<sub>2</sub>] Oxidation.**  $^1\text{H}$  NMR (CDCl<sub>3</sub>, 300 MHz):  $\delta$  1.27 (m, 3H), 2.34 (m, 1H), 2.62 (d,  $J = 14.2$  Hz, 1H), 3.32–2.96 (br m, 2H), 3.49 (m, 1H), 4.02 (d,  $J = 16.6$  Hz, 1H), 5.01–4.67 (br m, 3H), 5.12 (d,  $J = 13.9$  Hz, 1H), 5.45 (d,  $J = 16.2$  Hz, 1H), 7.94–7.73 (br m, 4H), 8.20 (m, 2H), 9.64 (m, 2H).

**X-ray Structure Determination.** A thin green plate of dimensions  $0.32 \times 0.11 \times 0.48$  mm was used for all X-ray experiments. The data collection was carried out on a Rigaku AFC6S diffractometer at  $-120$  °C using Mo K $\alpha$  radiation ( $\lambda = 0.71069$  Å). Unit cell dimensions were determined by applying the setting angles of 25 high-angle reflections. Intensities of three standard reflections were monitored during the data collection showing no significant variance. The intensities were corrected for absorption by using  $\psi$  scans of several reflections. The transmission factors ranged from 0.76 to 1.00. The structure was solved by direct methods (SIR92).<sup>84</sup> Calculations were performed on a Silicon Graphics Indigo 2 Extreme computer by employing the teXsan 1.7 software.<sup>85</sup> Full-matrix least-squares refinement with anisotropic thermal displacement parameters for the Cu, Cl, and F atoms yielded a final  $R$  of 0.057 ( $R_w = 0.078$ ). An inspection of a difference Fourier map indicated the presence of three weak peaks corresponding to a partially populated ethanol molecule. The non-hydrogen atoms of this molecule were refined isotropically with the occupancy of 0.5. The final difference map was essentially featureless with the highest peak of  $0.59$  e/Å<sup>3</sup>.

**Results and Discussion**

**Ligand Synthesis.** Ligands **1–4** were prepared from the diamines by condensation with aldehydes, followed by reduction of the resulting imines to secondary amines, and subsequent alkylation at the secondary nitrogen centers to give the desired quadridentate chelates (Scheme 1). Ligands are designated in

the following manner: diamine(alkyl group)terminal donor group. The diamine backbone is indicated first (en or *S*-pn), followed by the noncoordinating alkyl group given in parentheses (Bn or F<sub>5</sub>Bn) and then the terminal donor group (py = pyridine; qn = quinoline). The Schiff base precursor to ligands **1** and **2** was prepared by stirring ethylenediamine with 2 equiv of pyridinecarboxaldehyde in CH<sub>2</sub>Cl<sub>2</sub> containing molecular sieves. Filtration and concentration yielded the diimine products in high yield. While this approach works well for en backbone ligands, since *S*-pn is isolated as its di-HCl salt via an asymmetric synthesis starting from L-alanine methyl ester hydrochloride,<sup>82</sup> analogous Schiff base syntheses using *S*-pn to make ligands **3** and **4** required the prior liberation of the free base. This can be achieved using either concentrated basic solutions or a basic ion exchange column. Since these methods for generating the *S*-pn free base are somewhat tedious and they result in significant losses of product, a direct route was devised that involved the reaction of *S*-pn·2HCl with the desired aldehyde in the presence of excess base, i.e., triethylamine, in acetonitrile solution. After workup, the desired *S*-pn Schiff bases were obtained in good yield.

The Schiff bases were then reduced with sodium borohydride in methanol to yield quadridentates with secondary diamines at the internal donor positions.<sup>86,87</sup> This approach is more convenient than other reported methods using diborane<sup>83</sup> or reductions with Zn/HOAc<sup>42</sup> or Pd/C.<sup>88</sup> Reduction products were obtained relatively cleanly and in high yield. The final step of ligand synthesis involves alkylation of the secondary nitrogen centers to produce tertiary amines. Though reductive amination using formaldehyde and sodium cyanoborohydride works well for methylation,<sup>47</sup> this route is not effective for larger, bulkier aldehydes. Instead it was discovered that reaction of the 2° diamines with NaH in THF, followed by addition of benzyl bromide, C<sub>6</sub>H<sub>5</sub>CH<sub>2</sub>Br, or  $\alpha$ -bromo-2,3,4,5,6-pentafluorotoluene, C<sub>6</sub>F<sub>5</sub>CH<sub>2</sub>Br, resulted in the efficient formation of the desired alkylated products.<sup>89</sup> Most quadridentate ligands were used as prepared for making complexes. In certain cases, they were purified by chromatography or by conversion to their tetra-HCl salts followed by recrystallization.

**Synthesis and Characterization of Metal Complexes.** Metal complexes were prepared by combining alcohol solutions of the free ligands with those of the appropriate metal chloride, MCl<sub>*n*</sub> ( $n = 2$ , M = Mn, Fe, Co, Ni, Cu, Zn;  $n = 3$ , M = Fe). In a few cases (M = Mn and Ni), following literature precedent, the tetra-HCl salt of the en(F<sub>5</sub>Bn)py ligand was utilized in place of the free base. Since the *S*-pn(F<sub>5</sub>Bn)qn ligand, **4**, showed very limited solubility in methanol or ethanol, it was dissolved in a warm CH<sub>2</sub>Cl<sub>2</sub>/EtOH solvent mixture prior to addition of ethanol solutions of the metal salts. Immediate color changes indicative of complexation were observed in all cases. For certain ligand–metal combinations, namely for *S*-pn(F<sub>5</sub>Bn)py with M = Co, Mn, Ni, and Zn and en(F<sub>5</sub>Bn)py for M = Mn and Ni, complexes precipitated directly from the alcohol reaction medium. Soluble complexes were isolated by concentration in vacuo followed by crystallization using either vapor diffusion or layering techniques with the indicated two solvent systems. Crude

(84) Altomare, A.; Burla, M. C.; Camalli, G.; Cascarano, G.; Giacovazzo, C.; Guagliardi, A.; Polidori, G. *J. Appl. Crystallogr.* **1994**, *27*, 435.  
 (85) *teXsan 1.7. Crystal Structure Analysis Package*; Molecular Structure Corp.: The Woodlands, TX, 1992.

(86) For other examples of the use of NaBH<sub>4</sub> as the reductant to make ligands of this type, see: Toftlund, H.; Pedersen, E.; Yde-Andersen, S. *Acta Chem. Scand. A* **1984**, *38*, 693–7.

(87) Branca, M.; Checconi, P.; Pispisa, B. *J. Chem. Soc., Dalton Trans.* **1976**, 481–8 and references therein.

(88) Gruenwedel, D. W. *Inorg. Chem.* **1968**, *7*, 495–501.

(89) For examples of alternate preparations of related ligands see refs 41, 59, and Arulsamy, N.; Glerup, J.; Hazell, A.; Hodgson, D. J.; McKenzie, C.; Toftlund, H. *Inorg. Chem.* **1994**, *33*, 3023–5.

products were typically redissolved in either  $\text{CH}_2\text{Cl}_2$  or  $\text{CH}_3\text{-CN}$  and were precipitated using ethanol, diethyl ether, or, more rarely, hexanes. When it proved difficult to obtain crystalline materials, complexes were sometimes isolated as analytically pure powders by rapid precipitation from similar solvent combinations. Details pertaining to specific metal complexes are provided in the Experimental Section. In general it was our experience that complexes of Mn, Fe(II), Co, and Ni tended to be easier to isolate as crystalline or powdery solids than complexes of Zn, Cu, and Fe(III) throughout the ligand series. This was especially true for Cu and Fe(II) complexes of the more bulky quinoline bearing ligand, **4**, which appeared to be unstable. Certain iron complexes of related ligands are unstable as well.<sup>59</sup>

It should be noted that it was not possible to prepare the entire series of metal complexes for each of the ligands. Often analytical data for isolated materials did not correlate well with predicted structures. Especially puzzling was the fact that though many complexes of en(Bn)py, **1**, yielded beautifully crystalline materials, it was difficult to determine the compositions of these samples based upon CHN analytical data. This could be due to partial dissociation of halide ligands and the presence of fractional amounts of solvent(s) associated with complexes in the solid state, to solvent species, or to the presence of minor impurities that proved difficult to remove. Though we were unable to obtain complexes of satisfactory purity with certain ligand and metal combinations after screening a variety of different solvent systems and purification techniques, it may still be possible to achieve pure and stable quadridentate compounds if different metal salts (e.g. other halides, acetates) and solvents are employed. Only those samples for which elemental analyses correlate well with predicted products are included in the Experimental Section. Since diamagnetic Zn(II) complexes provide valuable information about metal complex structure,  $^1\text{H}$  NMR spectral data in  $\text{CDCl}_3$  solution are tabulated for all Zn complexes, regardless of analytical purity. Likewise,  $^1\text{H}$  NMR spectral data for Co(III) complexes generated in situ from Co(II) precursors are also provided. Metal complexes were routinely characterized by conductivity measurements, electronic absorption and IR spectroscopy, and cyclic voltammetry.

The FT-IR spectra of the ligands and complexes all contain major bands at approximately 1655, 1525, 1503, and 1124  $\text{cm}^{-1}$ . Free ligands **1–3** also exhibit pyridyl ring vibrations at  $\sim 1585\text{--}1590\text{ cm}^{-1}$ . These shift to higher energies upon complexation ( $\sim 1601\text{--}1611\text{ cm}^{-1}$ ). By comparison, for the free quinoline ligand, **4**, an absorption appears at 1596  $\text{cm}^{-1}$  and this shifts very little upon complexation (e.g. Co complex: 1603  $\text{cm}^{-1}$ ), which may correlate with weaker binding to this bulkier ligand. Complexes that precipitate with associated alcohol solvent typically exhibit OH stretches in the  $\sim 3400\text{--}3050\text{ cm}^{-1}$  range. The Fe(III) complex of **2** shows a peak at 843  $\text{cm}^{-1}$ , characteristic of the  $\text{PF}_6^-$  counterion. These observations are consistent with what has been observed previously for related complexes.<sup>43</sup> Additional details about the structure and properties of quadridentate metal complexes are provided below and are organized according to metal ion in reverse order from Zn to Mn.

**Zinc Complexes.** All Zn(II) complexes are white or pale yellow in color with UV/vis spectra exhibiting bands in the UV region attributable to ligand absorptions (Table 1).  $^1\text{H}$  and  $^{13}\text{C}$  NMR spectra, combined with conductivity data, reveal considerable information about the structure of Zn(II) complexes of the quadridentate ligand series. In chloroform solution, either single or major diastereomers (>95%) were obtained for Zn(II)

**Table 1.** UV/Vis Spectral Data (250–800 nm Range) for Ligands and Complexes in  $\text{CH}_3\text{CN}$  Solution

compd	wavelength (nm) <sup>a</sup>
en(Bn)py	262 (6300), 270 sh, 300 sh
en(F <sub>5</sub> Bn)py	262 (8500), 270 sh, 300 sh
S-pn(F <sub>5</sub> Bn)py	262 (7800), 270 sh, 300 sh
S-pn(F <sub>5</sub> Bn)qn	263 (9000), 303 (6000), 308 sh, 316 (7300)
Mn{en(Bn)py}Cl <sub>2</sub>	262 (8400), 269 sh
Mn{en(F <sub>5</sub> Bn)py}Cl <sub>2</sub>	262 (3400), 270 sh, 320 sh
Mn{S-pn(F <sub>5</sub> Bn)py}Cl <sub>2</sub>	264 (7200), 270 sh
Fe{en(Bn)py}Cl <sub>2</sub>	258 (10 000), 413 (1100)
Fe{en(F <sub>5</sub> Bn)py}Cl <sub>2</sub>	260 (8400), 338 (1900), 402 (1200)
Fe{S-pn(F <sub>5</sub> Bn)py}Cl <sub>2</sub>	260 (7900), 341 (1600), 398 (1200)
[Fe{en(F <sub>5</sub> Bn)py}Cl <sub>2</sub> ]PF <sub>6</sub>	256 (19 000), 265 sh, 300 sh, 376 (420)
Co{en(Bn)py}Cl <sub>2</sub>	258 (7100), 270 sh, 300 sh, 510 sh, 536 (24), 660 sh
Co{en(F <sub>5</sub> Bn)py}Cl <sub>2</sub>	260 (6400), 270 sh, 300 sh, 510 sh, 540 (33), 640 sh
Co{S-pn(F <sub>5</sub> Bn)py}Cl <sub>2</sub>	260 (8300), 270 sh, 300 sh, 536 (38), 660 sh
Co{S-pn(F <sub>5</sub> Bn)qn}Cl <sub>2</sub>	292 sh, 297 sh, 305 (7400), 317 (7600), 588 (210), 633 sh, 666 sh, 685 (240)
Ni{en(F <sub>5</sub> Bn)py}Cl <sub>2</sub>	258 (9400), 270 sh, 398 sh, 638 (16)
Ni{S-pn(F <sub>5</sub> Bn)py}Cl <sub>2</sub>	258 (16 000), 270 sh, 400 sh, 625 (23)
Cu{en(F <sub>5</sub> Bn)py}Cl <sub>2</sub>	262 (11 000), 290 (4500), 794 (97)
Cu{S-pn(F <sub>5</sub> Bn)py}Cl <sub>2</sub>	261 (20 000), 289 sh, 460 (75), 794 (260)
Zn{en(F <sub>5</sub> Bn)py}Cl <sub>2</sub>	264 (6000), 270 sh
Zn{S-pn(F <sub>5</sub> Bn)py}Cl <sub>2</sub>	264 (6300), 270 sh

<sup>a</sup>  $\epsilon_{\text{max}}$  values in parentheses ( $\text{M}^{-1}\text{ cm}^{-1}$ ); sh = shoulder.

complexes of all the ligands. Structural differences among Zn(II) complexes correlate with the degree of steric bulk surrounding the metal center. Our work with ligands **1–4** and others of this type<sup>75</sup> has revealed that all three features of the ligand—the diamine backbone, the pendant alkyl substituent, and the apical donor group—play a role.

Zinc complexes of ligands with ethylenediamine backbones and pyridyl donor groups, en(Bn)py, **1**, and en(F<sub>5</sub>Bn)py, **2**, adopt  $C_2$ -symmetric structures in  $\text{CDCl}_3$  solution as evidenced by their NMR spectra. The  $^1\text{H}$  and  $^{13}\text{C}$  spectra for  $[\text{Zn}\{\text{en}(\text{F}_5\text{Bn})\text{py}\}\text{Cl}_2]$  in  $\text{CDCl}_3$  are shown in Figure 6. This, combined with the fact that these complexes are nonconducting even in acetonitrile solution, is consistent with octahedral, cis  $\alpha$  structures in which both chlorides are coordinated. The Zn(II) complex of the S-pn backbone ligand, S-pn(F<sub>5</sub>Bn)py, **3**, is also present as a major diastereomer in  $\text{CDCl}_3$  solution. However, other species are also evident in trace amounts ( $\sim 5\%$ ). Since **3** bears a methyl group on the internal chelate ring backbone, the major isomer adopts a cis  $\alpha$  topology but the complex is not  $C_2$  symmetric. Most of the resonances in the aromatic region of the  $^1\text{H}$  and  $^{13}\text{C}$  spectra are relatively insensitive to the methyl group on the diamine backbone. Differences are greater in benzylic and aliphatic regions; here all proton and carbon signals for  $[\text{Zn}\{\text{S-pn}(\text{F}_5\text{Bn})\text{py}\}\text{Cl}_2]$  are unique. Aside from expected differences arising from the unsymmetrical S-pn backbone, Zn complexes of **1–3** give rise to very similar spectra. This suggests that they all possess the same cis  $\alpha$  topology for the sole or major isomers.

In addition to varying the diamine backbone, it was also of interest to us to see how differences in steric demand at the terminal donor positions of the quadridentate ligand influence metal geometry. Thus, a Zn(II) complex of S-pn(F<sub>5</sub>Bn)qn, **4**, was prepared for comparison. The  $^1\text{H}$  NMR of the Zn complex of S-pn(F<sub>5</sub>Bn)qn in chloroform solution suggests that one major isomer (>95%) is formed. However, the spectrum is complex, and all protons exhibit unique resonances. It is also interesting

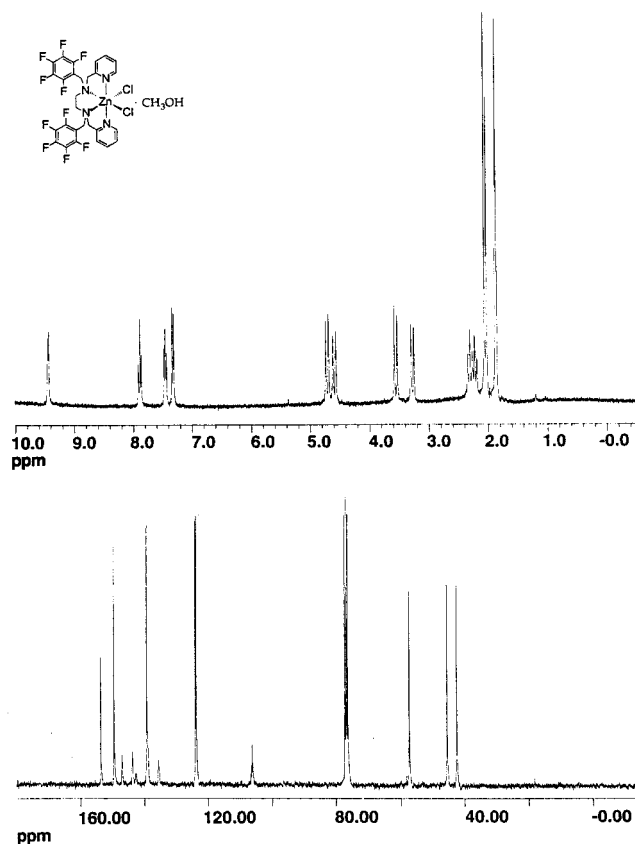


**Figure 6.**  $^1\text{H}$  ( $\text{CD}_3\text{CN}$ ) and  $^{13}\text{C}$  ( $\text{CDCl}_3$ ) NMR spectra of  $\text{Zn}\{\text{en}(\text{F}_5\text{-Bn})\text{py}\}\text{Cl}_2\cdot\text{MeOH}$ .

to note that the  $^1\text{H}$  NMR spectrum of this qn complex shares considerable overlap in the benzylic and aliphatic regions with a minor isomer evident in the spectrum of  $[\text{Zn}\{\text{S-pn}(\text{F}_5\text{Bn})\text{py}\}\text{Cl}_2]$ . Both complexes exhibit resonances at  $\sim 9.7$  ppm which, in our experience, seems to correlate with six coordinate structures. These observations, and comparison with data for *cis*  $\beta$  Co(III) complexes and  $^{13}\text{C}$  spectra of analogous bimetallic Zn complexes with *cis*  $\alpha$  and *cis*  $\beta$  topologies,<sup>41,43,50,61–64</sup> strongly point to a *cis*  $\beta$  assignment for the major isomer of  $[\text{Zn}\{\text{S-pn}(\text{F}_5\text{Bn})\text{qn}\}\text{Cl}_2]$ .<sup>50</sup> It should be noted, however, that both a nonideal *cis*- $\alpha$  structure, as was suggested by Rieger et al.<sup>59</sup> for a ferrous complex of a related but less bulky *en*(Me)qn ligand, and a five coordinate structure with one donor group dissociated, analogous to that seen for  $[\text{Cu}\{\text{en}(\text{F}_5\text{Bn})\text{py}\}\text{Cl}_2]$  in the solid state (Figure 7), are also consistent with the observed conductivity and NMR data.

Unlike the Zn(II) complexes of the *en* backbone ligands, those of *S-pn* ligands **3** and **4** give rise to more complex  $^1\text{H}$  NMR spectra upon dissolution in  $\text{CD}_3\text{CN}$ . New species emerge that are characterized both by the appearance of resonances in the 8–9 ppm and 3.5–4.6 ppm regions and the diminution of the downfield resonance at  $\sim 9.7$  ppm. Moreover, these complexes conduct to a small extent ( $\Lambda_{\text{M}} \sim 30 \Omega^{-1} \text{mol}^{-1} \text{cm}^2$ ) in  $\text{CH}_3\text{CN}$  solution. These observations suggest that a chloride ligand dissociates and either a five coordinate structure or a chloro-solvento species comprises a fraction of these samples. In summary, changes as subtle as the addition of a methyl substituent to the ethylenediamine backbone lead to observable differences in product distributions for Zn complexes of this family of quadridentate ligands. Whereas *en*-based ligands form single isomers, the *S-pn* systems show greater structural diversity in both polar and nonpolar solvents. This, combined with additional steric bulk at the terminal donor positions of these

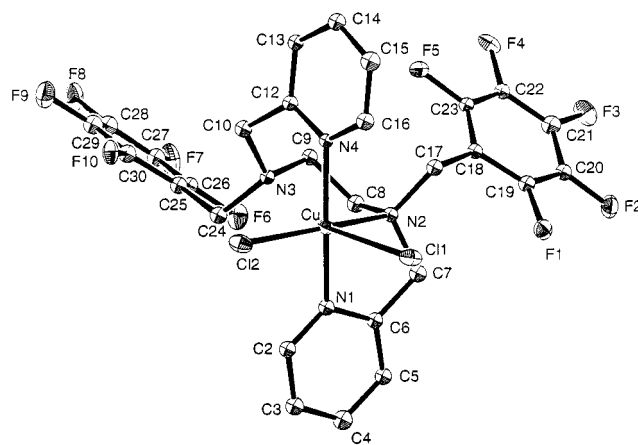


**Figure 7.** ORTEP drawing and labeling scheme for  $[\text{Cu}\{\text{en}(\text{F}_5\text{Bn})\text{py}\}\text{Cl}_2]$ . Ellipsoids are at 30% probability. Hydrogens are omitted for clarity.

ligands (qn vs py), may force a *cis*  $\beta$  topology in Zn complexes of the *S-pn*( $\text{F}_5\text{Bn}$ )qn ligand.

**Copper Complexes.** Copper complexes of the quadridentate ligands were typically isolated as green solids. Structural variation throughout the series of ligands for Cu(II) complexes is indicated by differences in color and conductivity in solution and by geometry in the solid state. In acetonitrile solution, complexes that are nonconducting or only slightly conducting (i.e. chlorides are coordinated in the inner sphere) tend to be green in color. Those in which chlorides are dissociated in a portion of the material are often blue-green or teal in color, whereas complexes from which the chloride ligands are removed using silver salts (e.g.  $\text{Ag}(\text{SbF}_6)$ ) generally form blue solutions in both polar ( $\text{CH}_3\text{CN}$ , MeOH) and noncoordinating ( $\text{CH}_2\text{Cl}_2$ ) solvents.<sup>42,75,90–93</sup> Likewise, complexes become more blue in color as the electronic and steric features of the ligand are varied. For example, acetonitrile solutions of Cu(II) complexes of *en*(Bn)py are green and nonconducting and those of the more electron deficient *en*( $\text{F}_5\text{Bn}$ )py and *S-pn*( $\text{F}_5\text{Bn}$ )py ligands are teal and slightly conducting, whereas a related ligand, *R,R*-*cn*( $\text{F}_5\text{Bn}$ )py with the bulkier *1R,2R*-diaminocyclohexane backbone,<sup>75</sup> is a 1:1 electrolyte and blue in color. These observations correlate well with predicted trends in the energy of d–d bands as the geometry at the Cu(II) center changes for a given ligand set<sup>75</sup> and may be compared to Cu complexes of related ligands.<sup>43,94,95</sup> Transitions are typically lower in energy (green) for distorted octahedral structures whereas square planar geometries typically give rise to higher energy transitions (blue). As is common for Cu(II) complexes, multiple Cu(II) species are likely present in acetonitrile solution as evidenced by complex UV/vis spectra and conductivities between values that would be expected for 1:1 electrolytes and nonconducting samples. This flexibility within the coordination sphere of Cu complexes has previously been described as the “plasticity effect”.<sup>96</sup> Moreover, as was seen in the solid state for  $[\text{Cu}\{\text{en}(\text{F}_5\text{Bn})\text{py}\}\text{Cl}_2]$ , it is also possible that both chlorides are bound

(90) Hathaway, B. J. *J. Chem. Soc., Dalton Trans.* **1972**, 1196–99.

(91) Hathaway, B. J.; Billing, D. E. *Coord. Chem. Rev.* **1970**, *5*, 143–207.

(92) *Comprehensive Coordination Chemistry*; Wilkinson, G., Ed.; Pergamon Press: Oxford, U.K., 1987; Vol. 5; Chapter 53, pp 533–774.

(93) Also see: Amundsen, A. R.; Whelan, J.; Bosnich, B. *J. Am. Chem. Soc.* **1977**, *99*, 6730–9.

(94) Nikles, D. E.; Powers, M. J.; Urbach, F. L. *Inorg. Chem.* **1983**, *22*, 3210–7.

(95) Sakurai, T.; Kimura, M.; Nakahara, A. *Bull. Chem. Soc. Jpn.* **1981**, *54*, 2976–8.



**Table 2.** Crystallographic Data for Cu{en(F<sub>5</sub>Bn)py}Cl<sub>2</sub>

chem formula	C <sub>29</sub> H <sub>23</sub> N <sub>4</sub> O <sub>0.5</sub> F <sub>10</sub> Cl <sub>2</sub> Cu
fw	759.96
space group	P2 <sub>1</sub> /a (No. 14)
a, Å	15.509(6)
b, Å	10.936(4)
c, Å	17.491(5)
$\beta$ , deg	96.53(3)
V, Å <sup>3</sup>	2947(1)
Z	4
T, °C	-120
$\lambda$ , Å	0.710 39
$\rho_{\text{calcd}}$ , g cm <sup>-3</sup>	1.71
$\mu(\text{Mo K}\alpha)$ , cm <sup>-1</sup>	10.17
R(F <sub>o</sub> ) <sup>a</sup>	0.057
R <sub>w</sub> <sup>a</sup>	0.078

$$^a R = (\sum |F_o| - |F_c|) / \sum |F_o|; R_w = [(\sum w(|F_o| - |F_c|)^2) / \sum w(F_o)^2]$$

**Table 3.** Selected Bond Lengths (Å) and Bond Angles (deg) for Cu{En(F<sub>5</sub>Bn)py}Cl<sub>2</sub>

(a) Bond Lengths			
Cu-Cl(1)	2.519(3)	Cu-Cl(2)	2.369(3)
Cu-N(1)	2.018(8)	Cu-N(2)	2.267(8)
Cu-N(3)	2.425(7)	Cu-N(4)	2.034(8)
(b) Bond Angles			
Cl(1)-Cu-Cl(2)	104.5(1)	Cl(1)-Cu-N(1)	89.4(2)
Cl(1)-Cu-N(2)	89.2(2)	Cl(1)-Cu-N(4)	95.5(2)
Cl(2)-Cu-N(1)	95.6(2)	Cl(2)-Cu-N(2)	164.8(2)
N(1)-Cu-N(4)	171.6(3)	N(2)-Cu-N(4)	95.3(3)

to give nonconducting solutions but that a nitrogen donor group may be dissociated to produce five coordinate structures overall.

The ORTEP diagram of the green Cu(II) complex, [Cu{en(F<sub>5</sub>Bn)py}Cl<sub>2</sub>], is shown in Figure 7. Crystallographic parameters are provided in Table 2, and selected bond lengths and bond angles are given in Table 3. The especially long Cu-N(3) distance of 2.425(7) Å suggests that a five coordinate square pyramidal structure with an N<sub>3</sub>Cl<sub>2</sub> donor set (an N(1)-N(2)-N(4)-Cl(2) base and a Cl(1) apical group) best describes the geometry of this compound in the solid state. Goodwin and Lions also proposed dissociation of a chelate donor group from Cu(II) centers to explain their observations with a related quadridentate ligand.<sup>42</sup> This structure may be contrasted with [Cu{en(H)py}Cl]<sup>+</sup>, a five-coordinate Cu(II) complex with an N<sub>4</sub>Cl donor set,<sup>97</sup> and also with a six coordinate Cu(II) complex of tn(H)py (tn = trimethylenediamine), a 5-6-5 chelate ring system with planar chelate coordination (i.e. N<sub>4</sub>Cl<sub>2</sub> donor set).<sup>98,99</sup> These solid-state examples illustrate that minor variations in the ligand can result in considerable structural differences in Cu complex geometry.<sup>96</sup> Though crystallographic analysis of metal complexes of chiral backbone ligands could provide valuable insights into the topology and stereospecificity of these systems, it proved difficult for us to grow crystals suitable for analysis using the S-pn backbone ligands, **3** and **4**.

**Nickel Complexes.** Nickel complexes were isolated as light green paramagnetic solids. All show very similar UV/vis spectra in CH<sub>3</sub>CN and CH<sub>2</sub>Cl<sub>2</sub> solutions with bands at ~630 and ~1080 nm typical for octahedral systems (Tables 1 and 4).<sup>100</sup> It should be noted that an additional band is present at ~400 nm as a

**Table 4.** Comparison of UV/Vis/NIR Spectral Data (250–1100 nm Range) for Nickel, Cobalt, and Iron Complexes of en(F<sub>5</sub>Bn)py and S-pn(F<sub>5</sub>Bn)py Ligands in Methylene Chloride Solution

compd	wavelength (nm)
Fe{en(F <sub>5</sub> Bn)py}Cl <sub>2</sub>	336 (1740), 407 (1420) <sup>a</sup>
Fe{S-pn(F <sub>5</sub> Bn)py}Cl <sub>2</sub>	335 (604), 406 (527) <sup>a</sup>
Co{en(F <sub>5</sub> Bn)py}Cl <sub>2</sub>	518 sh, 542 (37), 635 sh, 1086 (5)
Co{S-pn(F <sub>5</sub> Bn)py}Cl <sub>2</sub>	521 sh, 543 (37), 633 sh, 1084 (5)
Co{S-pn(F <sub>5</sub> Bn)qn}Cl <sub>2</sub>	300 sh, 307 (8400), 320 (8200), 540 sh, 601 (95), 613 (97), 635 (110), 669 (100), 809 sh
Ni{en(F <sub>5</sub> Bn)py}Cl <sub>2</sub>	402 (38), 642 (20), 1078 (11)
Ni{S-pn(F <sub>5</sub> Bn)py}Cl <sub>2</sub>	401 (41), 646 (21), 1083 (8)

<sup>a</sup> Long tail across visible region.

shoulder on a much stronger UV band in the spectra of all Ni complexes. Energies of absorptions for the Ni(II) complex of weaker field fluorinated ligands **2** and **3** appear at slightly lower energies than those for [Ni{en(Bn)py}Cl<sub>2</sub>]. Satisfactory analytical data were not obtained for the green crystalline [Ni{en(Bn)py}Cl<sub>2</sub>] complex; however, spectra were recorded for comparison. The following d-d transitions were observed: CH<sub>3</sub>CN, 394 sh, 629 nm; CH<sub>2</sub>Cl<sub>2</sub>, 393 sh, 631, 1062 nm. Though the complex [Ni{en(Bn)py}Cl<sub>2</sub>] is nonconducting in acetonitrile solution ( $\Lambda_M = 1.3 \Omega^{-1} \text{ mol}^{-1} \text{ cm}^2$ ), Ni complexes of fluorinated ligands, **2** and **3**, are slightly conducting in acetonitrile solutions ( $\Lambda_M = 22$  and  $33 \Omega^{-1} \text{ mol}^{-1} \text{ cm}^2$ , respectively). This suggests that chloride ligands dissociate from the Ni center in a portion of the sample in this polar solvent. A five coordinate Ni(II) species or six coordinate solvento-chloro or aquo-chloro species are all consistent with the observed conductivity data. No dramatic changes are observed in acetonitrile spectra as compared with those in methylene chloride that might be attributed to these new species that are formed. UV/vis spectra of Ni(II) complexes of related but stronger field secondary diamine ligands such as en(H)py with a variety of different ancillary ligands and counterions have been previously recorded for solids and in a variety of different solvents.<sup>43</sup> For these complexes, many of which are likely to be cis  $\alpha$  or even dimeric structures, d-d bands shift toward higher energies as expected (580 and 1000 nm for en(H)py vs 630 and 1080 nm for complexes of **2** and **3**).

**Cobalt Complexes.** Cobalt complexes of ligands **1–3** were isolated as lavender microcrystalline solids. Electronic absorption spectra in acetonitrile solution reveal absorptions at approximately 510, 538, and 650 nm indicative of six coordinate high-spin d<sup>7</sup> Co(II) centers for ligands **1–3** (Table 1).<sup>101</sup> Additional bands are present in the near-IR region at ~1085 nm (CH<sub>2</sub>Cl<sub>2</sub>) which are consistent with this assignment (Table 4). Conductivity data also support this assertion, as all complexes are essentially nonconducting ( $\Lambda_M < 10 \Omega^{-1} \text{ mol}^{-1} \text{ cm}^2$  in CH<sub>3</sub>CN). By comparison, the Co(II) complex of the more bulky S-pn(F<sub>5</sub>Bn)qn ligand, **4**, is slightly more bluish in color in the solid state. This is consistent with what has been seen previously for Co(II) complex with a related sterically bulky quinoline ligand.<sup>59</sup> Higher intensity bands at 588 and 685 nm ( $\epsilon = 210$  and  $240 \text{ L mol}^{-1} \text{ cm}^{-1}$ , respectively) in the UV/vis spectrum (CH<sub>3</sub>CN) of this quinoline complex along with a molar conductivity,  $\Lambda_M = 43 \Omega^{-1} \text{ mol}^{-1} \text{ cm}^2$ , suggest that chloride ligands are dissociated for a fraction of the sample. Most likely, mixtures of six and five coordinate species are present in

(96) Gazo, J.; Bersuker, I. B.; Garaj, J.; Kabesova, M.; Kohout, J.; Langfelderova, H.; Melnyk, M.; Serator, M.; Valach, F. *Coord. Chem. Rev.* **1976**, *19*, 253–97.

(97) Bailey, N. A.; McKenzie, E. D.; Worthington, J. M. *J. Chem. Soc., Dalton Trans.* **1973**, 1227–31.

(98) Pajunen, A.; Pajunen, S. *Acta Crystallogr.* **1986**, *C42*, 53–6.

(99) McKenzie, E. D.; Stephens, F. S. *Inorg. Chim. Acta* **1980**, *42*, 1–10.

(100) *Comprehensive Coordination Chemistry*; Wilkinson, G., Ed.; Pergamon Press: New York, 1987; Vol. 5, Chapter 50, pp 86–89.

(101) Lever, A. P. B. *Inorganic Electronic Spectroscopy*, 2nd ed.; Elsevier: New York, 1984; pp 480–505.

(102) Banci, L.; Bencini, A.; Benelli, C.; Gatteschi, D.; Zanchini, C. *Struct. Bonding* **1982**, *52*, 77ff.

solution.<sup>102</sup> Weak features present in the UV/vis spectrum of this complex in acetonitrile solution are more pronounced in the spectrum run in methylene chloride solution (Tables 1 and 4).

Though Co(II) complexes are paramagnetic, their oxidation to diamagnetic Co(III) systems allows for structural characterization by <sup>1</sup>H NMR and for comparison of these quadridentate ligand systems with analogous Co(III) systems.<sup>44–48</sup> A variety of different methods have been reported for the generation of Co(III) complexes with these types of quadridentate chelates, reaction with hydrogen peroxide in ethanol solution being the most common of these.<sup>46</sup> Unfortunately, our attempts to employ this standard preparation with ligands 1–4 met with little success. Reaction of CoCl<sub>2</sub>, en(Bn)py, and hydrogen peroxide yielded a blue-green solid, as expected by analogy with related systems; however, it did not precipitate readily from EtOH solution and was isolated by concentration instead. Inspection of products by <sup>1</sup>H NMR revealed chemical shifts consistent with what has been previously reported for analogous C<sub>2</sub> symmetric cis α systems<sup>46</sup> though resonances were broad. Hydrogen peroxide reactions with Co(II) chloride and the S-pn(F<sub>5</sub>Bn)qn ligand, 4, also exhibited the expected color changes; a green solid was obtained after partial concentration and precipitation with additional EtOH. However, as with the en(Bn)py ligand, 1, only broad resonances were observed, indicative of the presence of paramagnetic impurities. The Co(II) complex of en(F<sub>5</sub>Bn)py, 2, turned brown upon reaction with H<sub>2</sub>O<sub>2</sub>, and reaction of Co(II) with S-pn(F<sub>5</sub>Bn)py and H<sub>2</sub>O<sub>2</sub> resulted in the precipitation of the unreacted lavender Co(II) complex.

Lack of success with the standard methods prompted us to explore other common oxidants.<sup>103</sup> Reactions with Ag(OTf) did not generate significant quantities of the desired Co(III) products; however, reaction of Co(II) complexes with the stronger oxidant, bromine, did yield diamagnetic Co(III) products in all cases except for with the bulky ligand S-pn(F<sub>5</sub>Bn)qn, 4. The <sup>1</sup>H NMR spectrum of the oxidation product of [Co{en(F<sub>5</sub>Bn)py}Cl<sub>2</sub>] is provided as Supporting Information. It clearly reveals that a C<sub>2</sub>-symmetric cis α isomer was obtained. Cobalt complexes of other ligands also formed major isomers under these reaction conditions; however, all spectra bear evidence of at least one other minor product as well (<20% of the total sample as determined by integration). It should be noted that Br<sub>2</sub> may not be an innocent oxidant in these reactions. The bromide ion formed could exchange with the chloro compounds to generate new mixed-halide complexes. Moreover, it has been reported previously that dichlorocobalt(III) complexes with analogous quadridentate ligands are highly susceptible to hydrolysis; they rapidly form chloro-aquo species that are 2:1 electrolytes.<sup>46,104</sup> These various factors complicate product analysis and make it difficult to determine whether minor isomers are ancillary ligand byproducts, topological isomeric impurities, or some combination of the two.

**Iron Complexes.** Iron(II) complexes of en(F<sub>5</sub>Bn)py, S-pn(F<sub>5</sub>Bn)py, and en(Bn)py were isolated as canary yellow solids. Iron complexes of the bulky quinoline ligand, 4, were not amenable to synthesis by our standard preparations. Solutions turned orange and then dark brown upon reaction of the ligand with ferrous chloride, suggesting ready oxidation to Fe(III) products. Others have reported that the iron complex of a related nonfluorinated ligand, namely en(Bn)qn, was also susceptible to degradation in the presence of water and other solvents.<sup>59</sup>

Though some investigators have used this sensitivity to oxidation to synthetic advantage, no such Fe complexes were isolated with the quinoline ligand, 4. In contrast, the Fe(II) complexes of 1–3 showed no evidence of sensitivity to oxidation in solution or in the solid state. This is consistent with the observations of Hazell et al., who have noted that quadridentates with tertiary amine donors help to stabilize the lower Fe(II) oxidation state whereas ligands with stronger field secondary amines in the internal donor positions are sometimes prone to oxidative dehydrogenation, thus forming purple products.<sup>105</sup> For en(F<sub>5</sub>Bn)py, an Fe(III) complex was also readily prepared by reaction of the ligand with FeCl<sub>3</sub> followed by addition of NH<sub>4</sub>PF<sub>6</sub> to precipitate the product, [Fe{en(F<sub>5</sub>Bn)py}Cl<sub>2</sub>]PF<sub>6</sub>, as canary yellow plates. This complex is a 1:1 electrolyte in acetonitrile solution, consistent with an octahedral geometry at the metal center. The electronic absorption spectrum of this complex is similar to that observed for a related Fe(III) complex, [Fe(en(Me)py)Cl<sub>2</sub>]ClO<sub>4</sub>.<sup>52</sup> Likewise, the cis β Fe(III) complex [Fe{tn(H)py}Cl<sub>2</sub>]ClO<sub>4</sub> (tn = trimethylenediamine) prepared by Busch and co-workers was isolated as yellow prisms.<sup>106</sup> The other ligands were not amenable to Fe(III) complex synthesis; brown solids were often obtained. Though no structural information was obtained for these paramagnetic species, Fe(II) and Fe(III) complexes of related quadridentate ligands with pyridyl or quinoline and 3° donors all possess cis α structures in both monometallic and bimetallic complexes.<sup>51,59,107</sup> Complexes previously prepared by others have found application as bioinorganic models<sup>51,52,107</sup> and catalysts,<sup>59,108</sup> and they have been used in studies of spin equilibria in diisothiocyanate complexes.<sup>86,87</sup>

**Manganese Complexes.** Reaction of MnCl<sub>2</sub> with quadridentate ligands 1–4 produced off-white paramagnetic solids in high yield. White Mn(II) complexes of analogous ligands have been described previously as intermediates in the synthesis of bimetallic complexes<sup>53</sup> including many mixed valence species intended to model biological systems or for studying magnetic interactions between bridging ligands.<sup>109–112</sup> However, no characterization of these intermediates was provided. Related bimetallic Mn complexes have been utilized as oxidation catalysts.<sup>108</sup> As expected for high-spin d<sup>5</sup> systems, electronic absorption spectra of manganese complexes show ligand bands but no absorptions attributable to d–d transitions. A magnetic moment of 6.1 μ<sub>B</sub> was determined for [Mn{en(Bn)py}Cl<sub>2</sub>] using the Evans NMR method. This is somewhat higher than the spin only value of 5.9 μ<sub>B</sub> calculated for this d<sup>5</sup> system.

**Electrochemistry.** Cyclic voltammetry is a useful technique for assessing the purity of samples and for probing the electronic features of metal complexes. Methylene chloride solutions of the complexes and ligands were investigated using a glassy carbon working electrode, an aqueous silver/silver chloride reference electrode, and tetra-*n*-butylammonium hexafluorophosphate (TBAH) as the supporting electrolyte. Data are collected in Table 5. Free diamine ligands undergo oxidation

(103) Connelly, N. G.; Geiger, W. E. *Chem. Rev.* **1996**, *96*, 877.

(104) Also see: Henderson, R. A.; Tobe, M. L. *Inorg. Chem.* **1977**, *16*, 2576–83.

(105) See compound 8 found in the Experimental Section of ref 52.

(106) Alcock, N. *Acta Crystallogr., Sect. C* **1997**, *C53*, 1385–7.

(107) Arulsamy, N.; Goodson, P. A.; Hodgson, D. J.; Glerup, J.; Michelsen, K. *Inorg. Chim. Acta* **1994**, *216*, 21–29.

(108) Tetard, D.; Verlhac, J. *J. Mol. Catal. A: Chem.* **1996**, *113*, 223–30.

(109) Goodson, P. A.; Glerup, J.; Hodgson, D. J.; Michelsen, K.; Weihe, H. *Inorg. Chem.* **1991**, *30*, 4909–14 and references therein.

(110) Arulsamy, N.; Glerup, J.; Hazell, A.; Hodgson, D. J.; McKenzie, C. J.; Toftlund, H. *Inorg. Chem.* **1994**, *33*, 3023–4.

(111) Manchanda, R.; Thorp, H. H.; Brudvig, G. W.; Crabtree, R. H. *Inorg. Chem.* **1991**, *30*, 494–7.

(112) For a related monometallic Mn system with a N<sub>4</sub>O<sub>2</sub> donor set see: Neves, A.; Erthal, S. M. D.; Vencato, I.; Ceccato, A. S.; Mascarenhas, Y. P.; Nascimento, O. R.; Horner, M.; Batista, A. A. *Inorg. Chem.* **1992**, *31*, 4749–55.

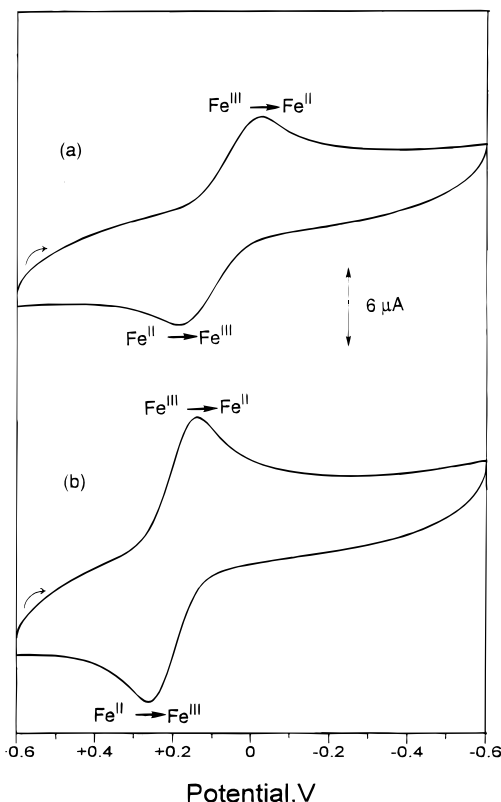
**Table 5.** Cyclic Voltammetric Data<sup>a</sup>

compd	$E_{p,a}$ (V)	$E_{p,c}$ (V)	$E_{1/2}$ (V)	$\Delta E_p^b$ (mV)
en(Bn)py	+1.05			
en(F <sub>5</sub> Bn)py	+1.08			
S-pn(F <sub>5</sub> Bn)py	+1.28	-1.24		
S-pn(F <sub>5</sub> Bn)qn	+1.06			
Mn{en(Bn)py}Cl <sub>2</sub>	+0.95	+0.86	+0.91	90
Mn{en(F <sub>5</sub> Bn)py}Cl <sub>2</sub>	+1.08	+1.00	+1.04	90
Mn{S-pn(F <sub>5</sub> Bn)py}Cl <sub>2</sub>	+1.09	+1.00	+1.04	90
Fe{en(Bn)py}Cl <sub>2</sub>	+0.40	+0.32	+0.36	85
Fe{en(F <sub>5</sub> Bn)py}Cl <sub>2</sub>	+0.48	+0.41	+0.44	75
Fe{en(Bn)py}Cl <sub>2</sub> <sup>c</sup>	+0.18	-0.019	+0.082	202
Fe{en(F <sub>5</sub> Bn)py}Cl <sub>2</sub> <sup>c</sup>	+0.26	+0.15	+0.20	112
[Fe{en(F <sub>5</sub> Bn)py}Cl <sub>2</sub> ]PF <sub>6</sub>	+0.46	+0.39	+0.42	70
Fe{S-pn(F <sub>5</sub> Bn)py}Cl <sub>2</sub>	+0.54	+0.45	+0.49	95
Co{en(Bn)py}Cl <sub>2</sub>	+0.77	+0.12 <sup>d</sup>		
Co{en(F <sub>5</sub> Bn)py}Cl <sub>2</sub>	+0.86	+0.26 <sup>d</sup>		
Co{S-pn(F <sub>5</sub> Bn)py}Cl <sub>2</sub>	+0.89	+0.26 <sup>d</sup>		
Co{S-pn(F <sub>5</sub> Bn)qn}Cl <sub>2</sub>		featureless		
Ni{en(F <sub>5</sub> Bn)py}Cl <sub>2</sub>	+1.40	+1.34	+1.37	65
Ni{S-pn(F <sub>5</sub> Bn)py}Cl <sub>2</sub>	+1.46	+1.36	+1.41	97
Cu{en(F <sub>5</sub> Bn)py}Cl <sub>2</sub>	+0.06	-0.11	-0.02	160
Cu{S-pn(F <sub>5</sub> Bn)py}Cl <sub>2</sub>	+1.25	-0.09 <sup>e</sup>		
Zn{en(F <sub>5</sub> Bn)py}Cl <sub>2</sub>		featureless		
Zn{S-pn(F <sub>5</sub> Bn)py}Cl <sub>2</sub>	+1.28			

<sup>a</sup> Instrumentation: BAS model CV-27 electrochemical analyzer. Working electrode: glassy carbon. Reference electrode: aqueous Ag/AgCl. Concentration: 0.5 mM. Supporting electrolyte: 0.1 M TBAH in CH<sub>2</sub>Cl<sub>2</sub>. Scan rate: 200 mV/s.  $E_{1/2}$  for the ferrocenium/ferrocene couple is at +0.47 V vs Ag/AgCl under these experimental conditions. <sup>b</sup>  $\Delta E_p$  is defined here as  $E_{p,a} - E_{p,c}$ . <sup>c</sup> As in (a) with the following exceptions: Instrumentation: BAS model CV-50W electrochemical analyzer. Reference electrode: Ag/AgCl in CH<sub>3</sub>CN. Scan rate: 100 mV/s.  $E_{1/2}$  for the ferrocenium/ferrocene couple is at +0.23 V vs Ag/AgCl under these experimental conditions. <sup>d</sup> Product wave. <sup>e</sup> Additional minor features present at +0.56 (anode) and +0.52 and +0.68 (cathode).

at high positive potentials (1.05–1.28 V), and for the S-pn(F<sub>5</sub>-Bn)py ligand, **3**, a reduction is also observed. It was of interest to us to determine which metal complexes exhibit reversible oxidations, as this could be important for certain catalytic reactions. For manganese, iron, and certain Cu complexes, quasireversible waves were observed. Manganese(II–III) couples appear at  $E_{1/2} \sim 0.91$ –1.04 V, whereas oxidation of Fe(II) to Fe(III) is more facile under similar experimental conditions ( $E_{1/2} \sim 0.36$ –0.49 V). While the CV of the Cu(II) complex of the bulky S-pn(F<sub>5</sub>Bn)qn ligand, **4**, contains a quasireversible oxidation, other copper complexes are not as well behaved. A series of weak oxidations and reductions are evident at different potentials, including ones at -0.43 V (vs ferrocene) indicative of free copper. This may be contrasted with the findings of Urbach and co-workers on related copper complexes, albeit with different solvent systems.<sup>94</sup> For Ni(II) complexes, weak quasireversible processes are evident at high potentials ( $\sim 1.4$  V). The Ni(III) oxidation state is typically highly unstable; often Ni(II)/Ni(III) oxidations occur in the range of +1 to +1.5 V.<sup>113–116</sup> As is expected for a d<sup>10</sup> system, Zn complexes are essentially featureless over the potential range under investigation.

For catalytic systems, it is desirable to be able to tune the electron richness of the metal center. Thus, determining whether, and to what extent, complexes of the fluorinated systems **2–4**

**Figure 8.** Comparison of the cyclic voltammograms for (a) [Fe{en(Bn)py}Cl<sub>2</sub>] and (b) [Fe{en(F<sub>5</sub>Bn)py}Cl<sub>2</sub>].

are more difficult to oxidize than analogous complexes of the nonfluorinated en(Bn)py ligand, **1**, is also important. The expected trends are clearly evident in  $E_{1/2}$  values for Mn and Fe complexes of ligands **1** and **2** that are identical except for perfluorination of the phenyl rings in **2**. For Mn, the fluorinated ligand is harder to oxidize by  $\sim 130$  mV whereas  $\Delta E_{1/2} = 80$  mV for the two Fe complexes in this series. Voltammograms of [Fe{en(Bn)py}Cl<sub>2</sub>] and [Fe{en(F<sub>5</sub>Bn)py}Cl<sub>2</sub>] that were recorded versus a nonaqueous Ag/AgCl reference electrode are compared in Figure 8.

Steric features of the ligands also influence how easily metal centers are oxidized. Few differences are observed between complexes of en(F<sub>5</sub>Bn)py, **2**, and S-pn(F<sub>5</sub>Bn)py, **3**; however, complexes of the bulky quinoline ligand may exhibit rather different electrochemistry, as is dramatically demonstrated for cobalt complexes. Complexes of the structurally similar ligands **1–3** undergo irreversible oxidations at 0.77–0.89 V; however, the voltammogram recorded for the Co complex of **4** is featureless throughout. The bulky quinoline ligand is less able to accommodate the contracted Co(III) oxidation state, perhaps due to unfavorable steric interactions between apical quinoline groups and equatorial chloro ligands that are undoubtedly necessary for stabilizing the octahedral geometry preferred by Co(III). Thus, [Co{S-pn(F<sub>5</sub>Bn)qn}Cl<sub>2</sub>] resists oxidation, both chemically, using common oxidants such as Br<sub>2</sub> or H<sub>2</sub>O<sub>2</sub>, and electrochemically.

## Conclusion

These investigations further demonstrate how readily the steric and electronic features of the amino–diimine family of ligands and their complexes may be varied. This, combined with the fact that appropriately designed ligands form C<sub>2</sub>-symmetric cis  $\alpha$  topologies and single (or major) diastereomers upon complexation to metal ions should make them well suited for

- (113) *Comprehensive Coordination Chemistry*; Wilkinson, G., Ed.; Pergamon Press: New York, 1987; Vol. 5, Chapter 50, p 287 ff.  
 (114) Freire, C.; de Castro, B. *Polyhedron* **1998**, *17*, 4227–35.  
 (115) Ward, M. S.; Shepherd, R. E. *Inorg. Chim. Acta* **1999**, *286*, 197–206.  
 (116) Bhattacharyya, S.; Weakley, T. J. R.; Chaudhury, M. *Inorg. Chem.* **1999**, *38*, 633–8.

applications in asymmetric catalysis. While metals such as Fe, Co, and Mn seem to adopt similar geometries throughout most of the ligand series, other metals such as Zn, Cu, and, to some extent, Ni are far more sensitive to the steric and electronic features of the ligand and can assume six, five, or even four coordinate structures. These differences could be exploited in reaction optimization. Moreover, varying the ancillary ligands from halides to other species, or replacing some or both of them with noncoordinating counterions, opens up even more possibilities for tailoring reactivity. Once complexes are proven viable catalysts for specific transformations, considerably more work is merited on these systems. Devising alternate routes to complexes that were difficult to access by standard preparations reported herein and further varying the steric and electronic features of these ligands, as well as more detailed characterization, are all worth pursuing. Recently we have utilized Cu complexes of this family of ligands as catalysts for the controlled polymerization of methyl methacrylate.<sup>117</sup> We have also seen moderate enantioselectivities using Cu complexes of chiral quadridentate ligands as catalysts for the Mukaiyama aldol

(117) Ng, C.; Johnson, R. M.; Samson, C. M. C.; Fraser, C. L. Unpublished manuscript.

reaction.<sup>75</sup> Rieger has described their potential to serve as catalysts for olefin polymerization.<sup>59</sup> Yet these few examples barely begin to explore the potential of cis  $\alpha$  complexes as catalysts. Numerous other reactions including oxidations, polymerizations, and Lewis acid-catalyzed transformations are ripe for exploration.

**Acknowledgment.** We gratefully acknowledge Dupont for a Young Professor Grant, the Alfred P. Sloan Foundation for a Research Fellowship, and the University of Virginia for support for this research. Dr. Daniel Derringer, Janet Cho, Scott A. Savage, and Laura E. Johnston are thanked for their various contributions to this project. C.L.F. also expresses her gratitude to Prof. B. Bosnich, who acquainted her with principles of inorganic stereochemistry and other factors important in chiral catalyst design.

**Supporting Information Available:** A <sup>1</sup>H NMR spectrum (300 MHz, CDCl<sub>3</sub>) for [Co{en(F<sub>5</sub>Bn)py}Cl<sub>2</sub>]Br·<sup>1</sup>/<sub>2</sub>CH<sub>3</sub>CH<sub>2</sub>OH·<sup>1</sup>/<sub>2</sub>CH<sub>2</sub>Cl<sub>2</sub> and IR spectral data for ligands and complexes measured as Nujol mulls (2 pages). An X-ray crystallographic file in CIF format for [Cu{en(F<sub>5</sub>Bn)py}Cl<sub>2</sub>]. This material is available free of charge via the Internet at <http://pubs.acs.org>.

IC990475V